Chapter 2
Ultralight Bosonic Dark Matter Theory

Derek F. Jackson Kimball, Leanne D. Duffy, and David J. E. Marsh

Abstract The basic theoretical concepts motivating the hypothesis that dark matter may consist of ultralight spin-0 or spin-1 bosons are explored. The origin of bosons with masses $\ll 1$ eV from spontaneous and explicit symmetry breaking is illustrated with examples. The origins and characteristics of nongravitational couplings or "portals" between ultralight bosons and Standard Model particles and fields are considered, with particular attention paid to the cases of the axion-photon and axion-fermion interactions. Theoretical motivations for the existence of ultralight bosons, besides as an explanation of dark matter, are examined, with particular focus on the Peccei-Quinn solution to the strong CP problem (resulting in the QCD axion) and a dynamical solution to the hierarchy problem (the "relaxion" hypothesis, based on a particular axion-Higgs coupling in the early universe). Mechanisms for non-thermal production of ultralight bosonic dark matter are examined.

2.1 Introduction

This book explores the hypothesis that dark matter consists predominantly of ultralight bosons. In this chapter we discuss the theoretical motivation for the ultralight bosonic dark matter (UBDM) hypothesis and the testable predictions

The original version of the chapter has been revised. A correction to this chapter can be found at https://doi.org/10.1007/978-3-030-95852-7_11

D. F. Jackson Kimball (✉)
Department of Physics, California State University, East Bay, Hayward, CA, USA
e-mail: derek.jacksonkimball@csueastbay.edu

L. D. Duffy
Los Alamos National Laboratory, Los Alamos, NM, USA
e-mail: ldd@lanl.gov

D. J. E. Marsh
Department of Physics, King's College London, London, UK
e-mail: david.j.marsh@kcl.ac.uk

D. F. Jackson Kimball, K. van Bibber (eds.), *The Search for Ultralight Bosonic Dark Matter*, https://doi.org/10.1007/978-3-030-95852-7_2

derived from it, considering a number of relevant examples along the way. At the outset several questions naturally arise:

- If we suppose that dark matter is a bosonic field, how do we describe that from a theoretical perspective?
- Why would such bosons be "ultralight"—with masses $\ll 1$ eV$/c^2$?
- How could such ultralight bosonic matter interact with known Standard Model particles and fields?
- Why should one expect that there exist bosons beyond those already discovered (e.g., photons, gluons, W and Z-bosons, and the Higgs boson)?
- How could ultralight bosons be created in the early universe in sufficient abundance to match the dark matter density observed today?

2.2 Bosonic Field Lagrangians

From the perspective of both classical and quantum field theory (QFT), a common place to begin trying to understand the physics of a new particle is to write down the Lagrangian (or more specifically, the Lagrangian density $\mathcal{L}$) of the corresponding field. The following several sections draw heavily from textbooks on QFT, such as Refs. [1–5], which offer more detail and further explanation of many of the key points addressed. Let us start by assuming we are dealing with a scalar field $\phi(\boldsymbol{r}, t)$; the quantum excitations of the scalar field $\hat{\phi}(\boldsymbol{r}, t)$ are spin-0 bosons.[1] This choice is motivated both by simplicity and because axions and axionlike particles (ALPs), some of the most prominent dark matter candidates, are spin-0 bosons. Further motivation for considering scalar fields is derived from the discovery of the Higgs boson [6, 7], proving that elementary spin-0 bosons do indeed exist in nature [8].

The Lagrangian $\mathcal{L}$ describing the scalar field will naturally depend on the rate of change of ϕ in time, $\partial_0\phi = \partial\phi/\partial t$, and the derivative of ϕ with respect to the spatial coordinates, $\boldsymbol{\nabla}\phi$. (In this chapter we will use natural units where $\hbar = c = 1$, see the discussion of units and conversion factors in the prefatory material at the beginning of this text.) We require that $\mathcal{L}$ be Lorentz invariant, so we will build our Lagrangian from the four-derivative of ϕ,

$$\partial_\mu\phi = \frac{\partial\phi}{\partial x^\mu} = \left(\frac{\partial}{\partial t}, \boldsymbol{\nabla}\right)\phi\,, \tag{2.1}$$

$$= \left(\frac{\partial\phi}{\partial t}, \frac{\partial\phi}{\partial x}, \frac{\partial\phi}{\partial y}, \frac{\partial\phi}{\partial z}\right), \tag{2.2}$$

which is manifestly Lorentz invariant. In the following we use the Einstein summation convention for repeated indices, with Greek indices such as μ running from $0 \rightarrow 3$, where 0 indicates the time-like component and 1, 2, and 3 are the spacelike components. The metric tensor describing flat spacetime is

[1] The "hat" on the scalar field denotes that we treat $\hat{\phi}$ as an operator.

$$g_{\mu\nu} = \begin{pmatrix} 1 & 0 & 0 & 0 \\ 0 & -1 & 0 & 0 \\ 0 & 0 & -1 & 0 \\ 0 & 0 & 0 & -1 \end{pmatrix} = \text{diag}\,[1, -1, -1, -1]\,, \tag{2.3}$$

which takes contravariant (upper) indices to covariant (lower) indices: $x_\mu = g_{\mu\nu}x^\nu$.

For simplicity, motivated at least in part by the principle of Occam's razor, we will also want to choose a form of $\mathcal{L}$ that depends on the lowest order of derivatives possible.[2] Since $\mathcal{L}$ is a scalar and $\partial_\mu\phi$ is a four-vector, at a minimum we must use the inner product of the four-derivatives of ϕ, and so our first guess at $\mathcal{L}$ is

$$\mathcal{L} = \frac{1}{2}\partial^\mu\phi\partial_\mu\phi = \frac{1}{2}\left(\partial_\mu\phi\right)^2\,, \tag{2.4}$$

$$= \frac{1}{2}\frac{\partial^2\phi}{\partial t^2} - \frac{1}{2}(\boldsymbol{\nabla}\phi)^2\,, \tag{2.5}$$

where the factor of $1/2$ is included to simplify future results, and we use the metric for flat spacetime. In analogy with the Lagrangian from classical mechanics describing particles, the term $(1/2)\left(\partial_\mu\phi\right)^2$ is often associated with a "kinetic" energy of the field.

So what can we learn from our guess for $\mathcal{L}$ about the properties of ϕ? By using Eq. (2.4) in the Euler–Lagrange equation,

$$\frac{\partial\mathcal{L}}{\partial\phi} - \partial_\mu\left(\frac{\partial\mathcal{L}}{\partial\left(\partial_\mu\phi\right)}\right) = 0\,, \tag{2.6}$$

noting that

$$\frac{\partial\mathcal{L}}{\partial\phi} = 0 \tag{2.7}$$

and

$$\frac{\partial\mathcal{L}}{\partial\left(\partial_\mu\phi\right)} = \partial^\mu\phi\,, \tag{2.8}$$

we find from Eq. (2.6) that

$$\partial_\mu\partial^\mu\phi = \frac{\partial^2\phi}{\partial t^2} - \nabla^2\phi = 0\,. \tag{2.9}$$

[2] In principle, theories with higher-order derivatives are possible, but are associated with non-local effects and causality violation. Models involving such higher-order derivatives include, for example, theories of modified gravity (see, e.g., Ref. [9]).

Note that Eq. (2.9) shows that $j^\mu = \partial^\mu \phi$ is a conserved current, since $\partial_\mu j^\mu = 0$. The conservation of the current j^μ is a consequence of the continuous *shift symmetry* of the Lagrangian under the transformation $\phi \to \phi + \text{constant}$, a result of Noether's theorem [10].

Equation (2.9) is a wave equation for ϕ and thus has solutions of the form

$$\phi(\boldsymbol{r}, t) = \varphi_0 e^{i(\boldsymbol{k}\cdot\boldsymbol{r} - \omega t)} , \tag{2.10}$$

where φ_0 is the amplitude of this particular mode of the scalar field, ω is the frequency, and $\boldsymbol{k}$ is the wave vector. In natural units, the frequency ω is equivalent to the energy E of ϕ, as can be derived by applying the energy operator $\hat{E} = i(\partial/\partial t)$ to $\phi(\boldsymbol{r}, t)$. Similarly, the wave vector $\boldsymbol{k}$ is equivalent to the momentum $\boldsymbol{p}$ of ϕ, as can be derived by applying the momentum operator $\hat{\boldsymbol{p}} = -i\nabla$ to $\phi(\boldsymbol{r}, t)$.

Substituting Eq. (2.10) into Eq. (2.9), we obtain the dispersion relation

$$\omega^2 = |\boldsymbol{k}|^2 , \tag{2.11}$$

or, equivalently,

$$E = |\boldsymbol{p}| . \tag{2.12}$$

What does Eq. (2.12) imply about our scalar field ϕ? One of the key ideas of QFT is that particles can be interpreted as quantum excitations of fields. The dispersion relation (2.12) thus implies that if the field ϕ has zero momentum, $|\boldsymbol{p}| = 0$, then it has zero energy, $E = 0$, which means the particles associated with ϕ have zero rest mass ($m = 0$). Note that, in fact, these considerations also apply to classical fields. The dispersion relation for a classical field defines a "mass" based on the curvature of the dispersion around $|\boldsymbol{k}| = 0$.

But in order to match the astrophysical observations discussed in Chaps. 1 and 3, the particles associated with ϕ must behave as cold dark matter and thus cannot be massless. To get a theory of particles with mass, we need to modify the Lagrangian density (2.5) so that there is some energy "cost" to having a non-vacuum field value. This can be done by adding to our Lagrangian a potential energy term that depends on ϕ such that

$$\mathcal{L} = \frac{1}{2}\left(\partial_\mu \phi\right)^2 - \frac{1}{2} m^2 \phi^2 , \tag{2.13}$$

where, again, the factor $m^2/2$ is chosen to obtain the correct units and with future results in mind, and the potential energy term has a minus sign since the Lagrangian is the kinetic minus the potential energy (thus the larger the field ϕ, the larger the potential energy). To show that our theory describes massive particles, we can re-derive the dispersion relation using $\mathcal{L}$ from Eq. (2.13). Since now

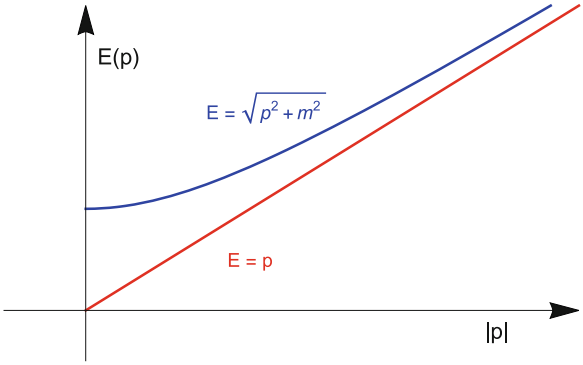

Fig. 2.1 Plot comparing the dispersion relation for a massless boson (red line) based on Eq. (2.12) with that for a massive boson (blue curve) based on Eq. (2.17). A key feature of the massive boson is the energy cost for zero-momentum excitations of the field, shown by the nonzero intercept of the dispersion curve on the energy axis

$$\frac{\partial \mathcal{L}}{\partial \phi} = -m^2 \phi \,, \tag{2.14}$$

the Euler–Lagrange equation (2.6) gives

$$\left(\partial_\mu \partial^\mu + m^2\right)\phi = 0 \,, \tag{2.15}$$

which is the Klein–Gordon equation. The solutions of the Klein–Gordon equation (2.15) are also of the form

$$\phi(\boldsymbol{r}, t) = \varphi_0 e^{-i(Et - \boldsymbol{p}\cdot\boldsymbol{r})} \,, \tag{2.16}$$

but with the dispersion relation

$$E^2 = |\boldsymbol{p}|^2 + m^2 \,, \tag{2.17}$$

which shows that if the field ϕ has zero momentum, $|\boldsymbol{p}| = 0$, then it has energy equal to the rest mass of the associated particle $E = m$. Thus the Lagrangian in Eq. (2.13) describes a relatively simple model for massive particles that could be dark matter.

Figure 2.1 compares the dispersion relation for massless particles derived from Eq. (2.4) to that for massive particles derived from Eq. (2.13). Already we can note an interesting feature of the scalar field that will be repeatedly referenced throughout this text, namely that a nonrelativistic bosonic field, for which $|\boldsymbol{p}| \ll m$, oscillates at the Compton frequency: $\omega \approx m$.

2.3 Why New Bosons Might Be Ultralight

So far, from the considerations in Sect. 2.2, we have from Eq. (2.13) a model of a scalar field whose particles have mass m. But, as discussed in Chap. 1, the UBDM hypothesis suggests that the dark matter particles have masses $\lesssim 0.1$ eV (and even perhaps as small as $m \sim 10^{-22}$ eV!), a small value compared to most known Standard Model particles with nonzero masses.[3] This invites the question: from a theoretical perspective, why might we expect new bosons to be ultralight? One of the main motivations for postulating the existence of new bosons with ultralight masses comes from the physics of *spontaneous symmetry breaking*, which we explore in this section.

Let us reconsider our model Lagrangian for the scalar field,

$$\mathcal{L} = \frac{1}{2}\left(\partial_\mu \phi\right)^2 - V(\phi) \,, \tag{2.18}$$

where we designate $V(\phi)$ as the potential energy density term. In Eq. (2.13), we chose $V(\phi) = m^2\phi^2/2$, but in principle we could try other potentials and investigate the consequences. In fact, this is a familiar approach used throughout physics: one might imagine that the true potential describing nature is some complicated function of ϕ, but one can always Taylor expand such a function:

$$V(\phi) = \sum_{n=0}^{\infty} \frac{c_n}{n!}\phi^n \,, \tag{2.19}$$

where c_n are constants. As long as the series converges, the first few terms of the Taylor expansion (2.19) may offer a reasonable approximation for $V(\phi)$. With this in mind, let us consider the following potential:

$$V(\phi) = \frac{\mu^2}{2}\phi^2 + \frac{\lambda}{4!}\phi^4 \,, \tag{2.20}$$

where λ is a constant. In Eq. (2.20) we take only the first two terms with even powers of ϕ from the expansion (2.19) to keep $V(\phi)$ symmetric about $\phi = 0$, so that $V(\phi)$ is invariant under the transformation $\phi_0 \to -\phi_0$. Also note that truncating the series at the ϕ^4 term is convenient as it makes the theory renormalizable (see, for example, chapter 31 of Ref. [1]). The potential described by Eq. (2.20) is shown in the plot on the top in Fig. 2.2. The minimum of this potential at $\phi = 0$ corresponds to the vacuum state of the field and the quantum excitations of ϕ are bosons with mass $m = \mu$, as can be seen in the limit where $\phi \ll 1$, in which case $V(\phi) \to \mu^2\phi^2/2$ and thus matches the potential from Eq. (2.13).

[3] Neutrinos, of course, have nonzero but comparatively small masses: the sum of the three different mass eigenstates for neutrinos is $\lesssim 0.1$ eV [11].

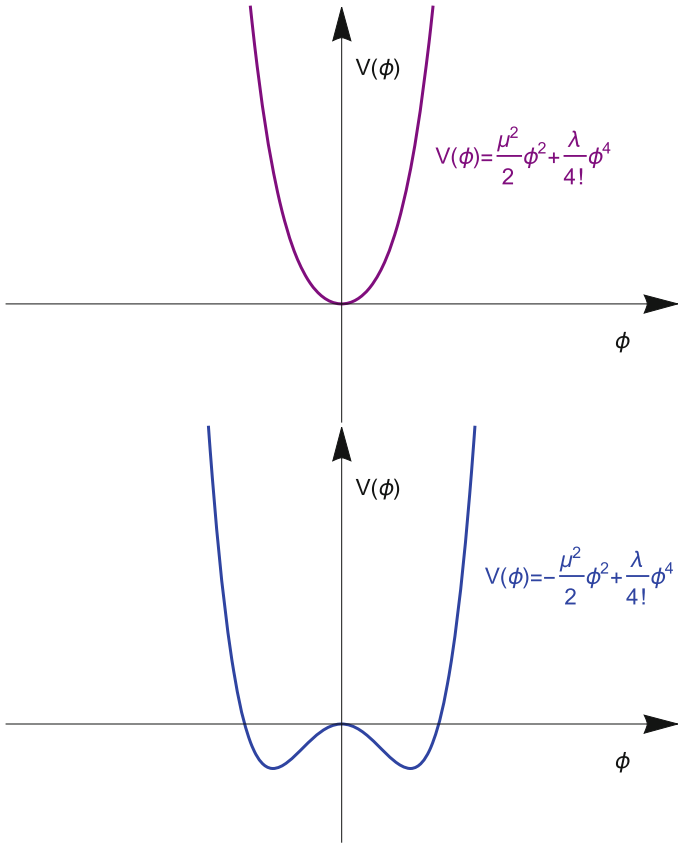

Fig. 2.2 The purple plot on the top shows a quartic scalar field potential $V(\phi)$ with a positive quadratic term [Eq. (2.20)], the blue plot on the bottom shows $V(\phi)$ with a negative quadratic term [Eq. (2.21)]

What if instead we construct a potential

$$V(\phi) = -\frac{\mu^2}{2}\phi^2 + \frac{\lambda}{4!}\phi^4 \,, \tag{2.21}$$

where the quadratic term is negative instead of positive? Then we get a shape of the potential as shown in the plot on the bottom in Fig. 2.2. Now there are two minima of the field at $\phi \neq 0$ (Problem 2.1). This means that the ground state of the field, which will be one of the two minima, *breaks reflection symmetry* and is not invariant under the transformation $\phi_0 \to -\phi_0$ (whereas, crucially, $V(\phi)$ still possesses reflection symmetry). This illustrates the essence of *spontaneous symmetry breaking* and

shows how the vacuum expectation value of the field acquires a nonzero amplitude (see Problem 2.1).

? Problem 2.1 Vacuum Field and Boson Mass in Spontaneous Symmetry Breaking

Solve for the minima of the potential $V(\phi)$ described by Eq. (2.21). These are the two possible vacua or "vacuum expectation values" of the field ϕ, both of which are nonzero. Thus the field ϕ has the property that even when there are no bosons present, the field is nonzero, possibly with relatively large amplitude. This is in contrast to the more familiar case of the electromagnetic field whose vacuum expectation value is zero, so that where there are no photons present the average electromagnetic field is zero. Also find the new mass of the boson.

Solution on page 309.

Still we have not yet seen why bosons associated with the field ϕ might be ultralight. Let us introduce a new model, this time with two different scalar fields, $\alpha(\boldsymbol{r}, t)$ and $\beta(\boldsymbol{r}, t)$. We construct a potential for these two scalar fields similar to that from Eq. (2.21):

$$V(\alpha, \beta) = -\frac{\mu^2}{2}\left(\alpha^2 + \beta^2\right) + \frac{\lambda}{4!}\left(\alpha^2 + \beta^2\right)^2 . \tag{2.22}$$

The potential $V(\alpha, \beta)$, plotted in Fig. 2.3, possesses what is known as a global $\mathbb{SO}(2)$ symmetry: it is invariant with respect to rotations in the α-β plane. It is a *global symmetry* because in order to maintain invariance with respect to the transformation, the fields at all points in spacetime must be rotated in the same way in the α-β plane. The label $\mathbb{SO}(2)$ for the symmetry originates from group theory: "$\mathbb{SO}$" refers to the special orthogonal group, namely the group of all orthogonal matrices[4] whose determinants $= 1$ (this condition is what makes this subgroup of all orthogonal matrices "special"). $\mathbb{SO}(2)$ is the special orthogonal group of 2×2 matrices, equivalent to the group of rotations about a point in two dimensions.

Now, instead of two potential minima as in the case of $V(\phi)$ from Eq. (2.21) (see Problem 2.1), there are an infinite number of minima on a ring of radius $\rho_0 = \sqrt{\alpha^2 + \beta^2} = \sqrt{6\mu^2/\lambda}$ centered at $(\alpha = 0,\ \beta = 0)$. This is seen by writing Eq. (2.22) in terms of $u = \alpha^2 + \beta^2$,

$$V(u) = -\frac{\mu^2}{2}u + \frac{\lambda}{4!}u^2 , \tag{2.23}$$

[4] An orthogonal matrix is a matrix whose inverse equals its transpose.

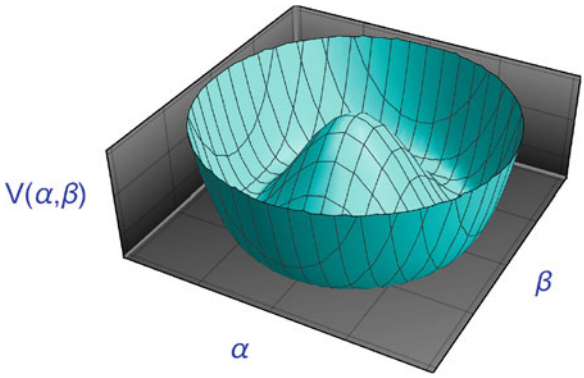

Fig. 2.3 Plot of the potential $V(\alpha, \beta)$ from Eq. (2.22)

and then finding the minimum with respect to u:

$$\left[\frac{\partial V}{\partial u}\right]_{u=u_{\min}} = -\frac{\mu^2}{2} + \frac{\lambda}{12}u_{\min} = 0 \tag{2.24}$$

$$\Rightarrow u_{\min} = \frac{6\mu^2}{\lambda}\,. \tag{2.25}$$

What happens when this system undergoes spontaneous symmetry breaking? Suppose the system "falls into" a particular ground state of the system. Without loss of generality, let us choose the ground state ($\alpha = \alpha_0 = \sqrt{6\mu^2/\lambda},\ \beta = \beta_0 = 0$). In order to investigate small perturbations around this particular field minimum, we can re-write the Lagrangian in terms of the variables

$$\bar{\alpha} \equiv \alpha - \alpha_0 = \alpha - \sqrt{\frac{6\mu^2}{\lambda}}\,, \tag{2.26}$$

$$\bar{\beta} \equiv \beta - \beta_0 = \beta\,, \tag{2.27}$$

noting that

$$\partial_\mu \bar{\alpha} = \partial_\mu \alpha\,, \tag{2.28}$$

$$\partial_\mu \bar{\beta} = \partial_\mu \beta\,. \tag{2.29}$$

The Lagrangian with the potential from Eq. (2.22), written in terms of $\bar{\alpha}$ and $\bar{\beta}$, is given by

$$\mathcal{L} = \frac{1}{2}\left(\partial_\mu \bar{\alpha}\right)^2 + \frac{1}{2}\left(\partial_\mu \bar{\beta}\right)^2 + \frac{\mu^2}{2}\left[(\bar{\alpha}+\alpha_0)^2 + \bar{\beta}^2\right] - \frac{\lambda}{4!}\left[(\bar{\alpha}+\alpha_0)^2 + \bar{\beta}^2\right]^2\,, \tag{2.30}$$

which is equivalent to

$$\begin{aligned}\mathcal{L} =& \frac{1}{2}\left(\partial_\mu \bar{\alpha}\right)^2 + \frac{1}{2}\left(\partial_\mu \bar{\beta}\right)^2 + \frac{3}{2}\frac{\mu^4}{\lambda} - \mu^2\bar{\alpha}^2 - \mu\sqrt{\frac{\lambda}{6}}\bar{\alpha}^3 - \frac{\lambda}{4!}\bar{\alpha}^4 \\ & - \frac{\lambda}{4!}\bar{\beta}^4 - \mu\sqrt{\frac{\lambda}{6}}\bar{\alpha}\bar{\beta}^3 - \frac{\lambda}{12}\bar{\alpha}^2\bar{\beta}^2 \,.\end{aligned} \tag{2.31}$$

? Problem 2.2 Lagrangian for Two Scalar Fields

Derive Eq. (2.31) from Eq. (2.30).

Solution on page 310.

The physics described by $\mathcal{L}$ is unchanged by resetting the zero of the potential, so the constant term in Eq. (2.31), $3\mu^4/(2\lambda^2)$, can be subtracted. As a first approximation, let us consider only small amplitude field excitations and therefore neglect terms higher than second order in the fields $\bar{\alpha}$, $\bar{\beta}$:

$$\mathcal{L} \approx \frac{1}{2}\left(\partial_\mu \bar{\alpha}\right)^2 + \frac{1}{2}\left(\partial_\mu \bar{\beta}\right)^2 - \mu^2\bar{\alpha}^2 \,. \tag{2.32}$$

The part of the Lagrangian describing the $\bar{\alpha}$ field has a form analogous to Eq. (2.13) and thus represents a field whose quantum excitations are bosons of mass $m = \sqrt{2}\mu$. The part of the Lagrangian describing the $\bar{\beta}$ field has a form analogous to Eq. (2.4) and thus represents a field whose quantum excitations are massless bosons. The $m = 0$ excitations of the $\bar{\beta}$ field are known as *Goldstone bosons* [12], massless bosons appearing whenever a continuous symmetry, in this case $\mathbb{SO}(2)$, is spontaneously broken (a consequence of Goldstone's theorem [13]). The reason that the $\bar{\beta}$ bosons are massless can be intuited from the shape of the potential plotted in Fig. 2.3, shown in an "overhead" view in Fig. 2.4. Small excitations of the $\bar{\beta}$ field (indicated by the double-headed purple arrow in Fig. 2.4) around the ground state (indicated by the purple dot in Fig. 2.4) occur essentially without any increase in potential energy, as they are along the ring of minima in the "trough" of the potential $V(\alpha, \beta)$. In contrast, excitations of the $\bar{\alpha}$ field are perpendicular to the double-headed purple arrow in Fig. 2.4, where the potential resembles that of a simple harmonic oscillator, corresponding to the massive bosons associated with the potential of Eq. (2.13).

So far, our model based on the potential from Eq. (2.22) shows no indication of an ultralight field: rather we have one field ($\bar{\alpha}$) that has an arbitrary mass and another field ($\bar{\beta}$) that is massless. The appearance of an ultralight field requires one more ingredient in our model: *explicit symmetry breaking* on top of the spontaneous symmetry breaking. By explicit symmetry breaking we mean that the global $\mathbb{SO}(2)$ symmetry of the potential $V(\alpha, \beta)$ of Eq. (2.22) is itself broken, so that $V(\alpha, \beta)$ is no longer symmetric with respect to rotations in the α-β plane. In theories proposing ultralight bosons, such explicit symmetry breaking occurs due to, for example, non-perturbative effects in quantum chromodynamics (QCD), leading to so-called "soft"

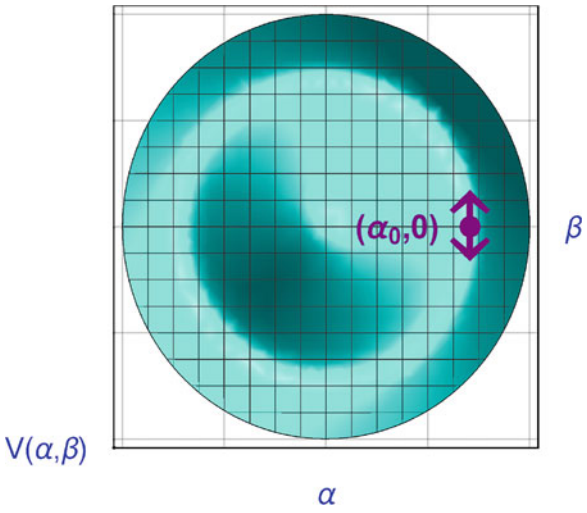

Fig. 2.4 Overhead view of the potential $V(\alpha, \beta)$ from Eq. (2.22). The purple dot indicates the (arbitrary) ground state after spontaneous symmetry breaking at ($\alpha = \alpha_0 = \sqrt{6\mu^2/\lambda},\ \beta = \beta_0 = 0$). The double-headed purple arrow indicates small perturbations of the β field around $\beta = \bar{\beta} = 0$, requiring approximately zero energy as seen from Eq. (2.32). Thus the quantum excitations of the β field are massless bosons, a consequence of Goldstone's theorem

explicit breaking of the symmetry (where "soft" refers to the fact that the symmetry is restored at high energy scales), or even effects associated with quantum gravity (which is generically expected to violate global symmetries), see the reviews [14–19] for further discussion. For the purposes of our present investigations, let us invoke explicit symmetry breaking of the potential by "tilting" $V(\alpha, \beta)$ toward the original vacuum state from the spontaneously broken symmetry (α_0, β_0) by adding the term

$$V_\epsilon = -\epsilon\lambda\alpha_0^3\alpha \tag{2.33}$$

to the potential of Eq. (2.22), so the Lagrangian is now

$$\mathcal{L} = \frac{1}{2}(\partial_\mu\alpha)^2 + \frac{1}{2}(\partial_\mu\beta)^2 + \frac{\mu^2}{2}\left(\alpha^2+\beta^2\right) - \frac{\lambda}{4!}\left(\alpha^2+\beta^2\right)^2 + \epsilon\lambda\alpha_0^3\alpha\ . \tag{2.34}$$

In Eqs. (2.33) and (2.34), $\epsilon \ll 1$ is a small parameter characterizing the symmetry breaking. Figure 2.5 shows a plot of the potential (the tilt is greatly exaggerated so as to be clearly visible).

The explicit symmetry breaking due to V_ϵ shifts the minimum of the potential with respect to α, as seen in Problem 2.3.

? Problem 2.3 Explicit and Spontaneous Symmetry Breaking

Keeping only terms to first order in ϵ, verify that the minimum of the potential in Eq. (2.34), namely

$$V(\alpha, \beta) = -\frac{\mu^2}{2}\left(\alpha^2+\beta^2\right) + \frac{\lambda}{4!}\left(\alpha^2+\beta^2\right)^2 - \epsilon\lambda\alpha_0^3\alpha\ , \tag{2.35}$$

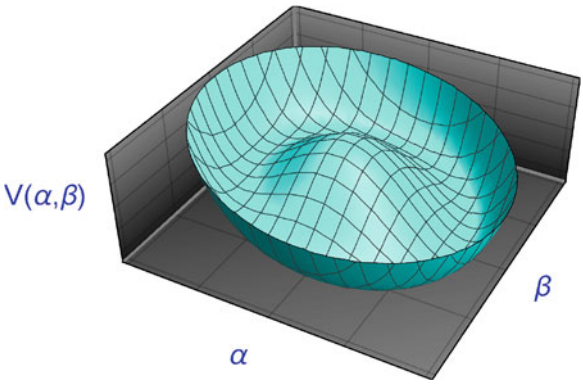

Fig. 2.5 Plot of the potential from Eq. (2.34), showing explicit symmetry breaking. The potential is tilted toward the original vacuum state (α_0, β_0) identified in Fig. 2.4

occurs at

$$\alpha = \alpha_0(1 + 3\epsilon) \,, \tag{2.36}$$

$$\beta = 0 \,, \tag{2.37}$$

where, as before, $\alpha_0 = \sqrt{6\mu^2/\lambda}$. Thus in order to investigate small perturbations around this particular field minimum, the Lagrangian (2.34) can be re-written in terms of the variable

$$\bar{a} = \alpha - \alpha_0(1 + 3\epsilon) \,. \tag{2.38}$$

By writing $\mathcal{L}$ in terms of $\bar{a}$, keeping only first order terms in ϵ and second order or smaller terms in the fields $\bar{a}$ and β, and also appropriately resetting the zero of the potential (allowing all constant terms to be subtracted), show that the potential (2.35) can be approximated as

$$V(\bar{a}, \beta) \approx \mu^2\bar{a}^2 + 3\epsilon\mu^2\beta^2 \,. \tag{2.39}$$

Solution on page 311.

Based on Eq. (2.39), the Lagrangian for the fields resulting from both spontaneous and explicit symmetry breaking can be approximately described as

$$\mathcal{L} = \frac{1}{2}\left(\partial_\mu\bar{a}\right)^2 + \frac{1}{2}\left(\partial_\mu\beta\right)^2 - \mu^2\bar{a}^2 - 3\epsilon\mu^2\beta^2 \,, \tag{2.40}$$

which shows that due to the explicit symmetry breaking, the β field has acquired a small mass $\propto \sqrt{\epsilon}$,

$$m_\beta^2 \approx 6\epsilon\mu^2 \,. \tag{2.41}$$

Thus β represents the sought-after ultralight bosonic field: the quantum excitations of the β field are commonly known as a *pseudo-Goldstone bosons* or *pseudo-Nambu-Goldstone bosons* (pNGBs in the literature, see, for example, Ref. [12]).[5]

In order to connect our somewhat simplistic model to more realistic UBDM scenarios, it is useful to re-parameterize the descriptions of the explicit and spontaneous symmetry breaking. We can associate a characteristic energy scale f with the spontaneous symmetry breaking based on the depth of the potential [see, e.g., Eqs. (2.23) and (2.25)],

$$|V_{\min}| \sim \frac{\mu^4}{\lambda^2} \sim f^4 \,, \tag{2.42}$$

where we note that $V(\alpha, \beta)$ represents an energy density and thus, in natural units, is proportional to the fourth power of energy. The energy scale Λ describing the explicit symmetry breaking can be characterized by the associated part of the potential [Eq. (2.33)], namely

$$|V_\epsilon| \approx \epsilon\lambda\alpha_0^4 \sim \epsilon\frac{\mu^4}{\lambda} \sim \Lambda^4 \,. \tag{2.43}$$

The mass of the β boson [Eq. (2.41)] can now be re-written in terms of f and Λ:

$$m_\beta^2 \sim \epsilon\mu^2 \sim \left(\epsilon\frac{\mu^4}{\lambda}\right) \times \left(\frac{\lambda}{\mu^2}\right) , \tag{2.44}$$

$$\sim \frac{\Lambda^4}{f^2} \,. \tag{2.45}$$

Since the mass of the β boson scales as $m \sim \Lambda^2/f$, if $f \gg \Lambda$ (which corresponds to ϵ being small), as is the case in many beyond-the-Standard-Model theories incorporating such effects, then indeed the new boson can be ultralight. Note that we have an additional symmetry restored in the limit where $\epsilon \to 0$, namely the $\mathbb{SO}(2)$ symmetry, and thus we say that the ultralight mass of the pseudo-Goldstone boson is "technically natural."

Specific models of ultralight bosons suggest particular values for the spontaneous symmetry breaking scale f and the explicit symmetry breaking scale Λ. For example, the spontaneous symmetry breaking might occur at the Planck scale, in which case $f \sim 10^{28}$ eV. A possible source of (soft) explicit symmetry breaking arises from the strong interaction, in which case the explicit symmetry breaking scale is given by the QCD confinement scale (the energy scale above which calculations of the strong coupling constant diverge), i.e., $\Lambda \sim 10^8$ eV. Employing

[5] Goldstone bosons resulting from spontaneous symmetry breaking are massless, while pseudo-Goldstone bosons, possessing relatively small but nonzero masses, result from the combination of spontaneous and explicit symmetry breaking as considered here.

these energy scales in Eq. (2.45) gives a boson mass of $m \sim 10^{-12}$ eV, which is much, much lighter than any Standard Model boson with nonzero mass.

Tutorial: Spontaneous and Explicit Breaking of the $\mathbb{U}(1)$ Symmetry of a Complex Scalar Field

In this tutorial, we offer another example elucidating the origin of an ultralight bosonic field from the combination of spontaneous and explicit symmetry breaking. Instead of the two real scalar fields α and β considered above, let us consider a single complex scalar field φ, where we can make the correspondence:

$$\varphi = \alpha + i\beta \, . \tag{2.46}$$

Then the Lagrangian corresponding to the potential in Eq. (2.22) can be written as

$$\mathcal{L} = \frac{1}{2}\left(\partial^{\mu}\varphi\right)^{\dagger}\left(\partial_{\mu}\varphi\right) + \frac{\mu^2}{2}\varphi^{\dagger}\varphi - \frac{\lambda}{4!}\left(\varphi^{\dagger}\varphi\right)^2 \, . \tag{2.47}$$

Next we can re-parametrize the complex field using polar coordinates:

$$\varphi = \rho e^{i\theta} \, , \tag{2.48}$$

which yields a new form for the Lagrangian (2.47):

$$\mathcal{L} = \frac{1}{2}\left(\partial_{\mu}\rho\right)^2 + \frac{1}{2}\rho^2\left(\partial_{\mu}\theta\right)^2 + \frac{\mu^2}{2}\rho^2 - \frac{\lambda}{4!}\rho^4 \, . \tag{2.49}$$

Note that the Lagrangian described by Eqs. (2.47) and (2.49) exhibits a global $\mathbb{U}(1)$ symmetry for φ, namely that a global transformation $\varphi \rightarrow \varphi e^{i\theta'}$ has no effect on $\mathcal{L}$. $\mathbb{U}(1)$ refers to the one-dimensional unitary group, i.e., complex numbers with magnitude $= 1$, and so the $\mathbb{U}(1)$ symmetry is a symmetry with respect to rotations in the complex plane. The correspondence between rotations in the complex plane for φ and rotations in the real α-β plane is a consequence of the fact that $\mathbb{U}(1)$ is isomorphic to $\mathbb{SO}(2)$.

Similarly to the case of the two real-valued fields α and β, minima of the potential occur in a ring with radius $\rho = \rho_0 = \sqrt{6\mu^2/\lambda}$. Let us assume that the $\mathbb{U}(1)$ symmetry is spontaneously broken such that $\rho \rightarrow \rho_0$ and $\theta \rightarrow 0$. Then we can re-write the Lagrangian in terms of $\bar{\rho} = \rho - \rho_0$, which, after some algebra, yields

$$\mathcal{L} = \frac{1}{2}\left(\partial_{\mu}\bar{\rho}\right)^2 + \frac{1}{2}\rho_0^2\left(\partial_{\mu}\theta\right)^2 - \mu^2\bar{\rho}^2 - \frac{\lambda}{6}\rho_0\bar{\rho}^3 - \frac{\lambda}{24}\bar{\rho}^4 + \left(\frac{\bar{\rho}^2}{2} + \rho_0\bar{\rho}\right)\left(\partial_{\mu}\theta\right)^2 \, , \tag{2.50}$$

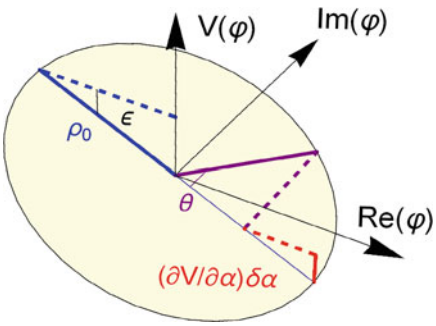

Fig. 2.6 Schematic diagram showing the effect of explicit symmetry breaking due to a tilt by an angle ϵ of the quartic potential for the complex scalar field φ (see Figs. 2.3 and 2.5 for illustrations of the analogous case for two real scalar fields, with and without tilt, respectively). The edge of the disk represents the ring of minima with respect to ρ at $\rho \approx \rho_0$ (radius ρ_0 shown by the solid blue line). If the potential is tilted by an angle ϵ, the potential acquires a θ-dependence given by $(\partial V/\partial\alpha)\delta\alpha$ (illustrated by the solid vertical red line). Here the solid purple radial line indicates a particular value of $\varphi = \rho_0 e^{i\theta}$, $\alpha = \mathrm{Re}(\varphi)$, $\delta\alpha \approx \rho_0(\cos\theta - 1)$ (illustrated by the dashed red line), and $\partial V/\partial\alpha = -\epsilon\mu^2\rho_0$

where in Eq. (2.50) we have dropped all constant terms, since they have no effect on the physics. Note that in Eq. (2.50), the terms independent of θ and linear in $\bar{\rho}$ have cancelled out, similarly to the derivation of Eq. (2.31) discussed in Problem 2.2. Retaining only second order or lower terms in $\bar{\rho}$ and θ, we obtain

$$\mathcal{L} \approx \frac{1}{2}\left(\partial_\mu \bar{\rho}\right)^2 + \frac{1}{2}\rho_0^2\left(\partial_\mu \theta\right)^2 - \mu^2\bar{\rho}^2 \,, \tag{2.51}$$

which is analogous to Eq. (2.32). Note that $\theta = \beta/\rho_0 \sim \beta/f$, where f is the spontaneous symmetry breaking scale defined in Eq. (2.43).

Next, we introduce explicit symmetry breaking by tilting the potential appearing in the Lagrangian (2.49) by an angle ϵ toward $\theta = 0$. Figure 2.6 illustrates the parametrization of the explicit symmetry breaking. The tilt by ϵ causes the potential to acquire a θ-dependence. For $\varphi = \rho_0 e^{i\theta}$, the real part of the field is $\mathrm{Re}(\varphi) = \alpha = \rho_0 \cos\theta$. The minimum of the tilted potential is at $\theta = 0$, and so the change in the potential with respect to the minimum is given by

$$\delta V(\theta) = \frac{\partial V}{\partial \alpha}\delta\alpha = \epsilon\mu^2\rho_0^2(1 - \cos\theta) \,, \tag{2.52}$$

where $\delta\alpha = -\rho_0(1 - \cos\theta)$. Including this term in the Lagrangian (2.51), we have

$$\mathcal{L} \approx \frac{1}{2}\left(\partial_\mu \bar{\rho}\right)^2 + \frac{1}{2}\rho_0^2\left(\partial_\mu \theta\right)^2 - \mu^2\bar{\rho}^2 - \epsilon\mu^2\rho_0^2(1 - \cos\theta) \,. \tag{2.53}$$

As a final step, to connect this result to the form of the potential most commonly encountered in the literature on UBDM, we use the relationships outlined in Eqs. (2.42), (2.43), and (2.45), along with the correspondence noted earlier, $\theta \sim \beta/f$, to write:

$$V(\beta) = m_b^2 f^2 \left[1 - \cos\left(\frac{\beta}{f}\right)\right] = \Lambda^4 \left[1 - \cos\left(\frac{\beta}{f}\right)\right]. \tag{2.54}$$

$V(\beta)$ can be expanded about $\beta = 0$ to give

$$V(\beta) \approx \frac{1}{2} m_b^2 \beta^2 \approx \frac{1}{2} \frac{\Lambda^4}{f^2} \beta^2 , \tag{2.55}$$

which can be compared to the β^2 term in Eq. (2.40).

End of Tutorial

2.4 Portals Between the Dark Sector and the Standard Model

The next major question we will address is how ultralight bosonic fields can interact nongravitationally with Standard Model particles and fields. To develop some intuition about such interactions, let us begin by continuing to work with our simple model of an ultralight bosonic field developed in Sect. 2.3. From a QFT perspective, interactions between two different fields arise when terms appear in the Lagrangian involving both fields as factors. In this way we can investigate interactions between the α (or $\bar{a}$) and β fields analyzed in Sect. 2.3. While the approximate Lagrangian of Eq. (2.40) has no such terms, they appear if we expand the Lagrangian of Eq. (2.34) to third order in the products of the fields, as shown in Problem 2.4.

? Problem 2.4 Interactions Between Two Scalar Fields

Using the results from the solution to Problem 2.3, expand the potential of Eq. (2.34) to third order in the products of the fields, thereby deriving two new "interaction" terms:

$$V_{\text{int}}(\bar{a}, \beta) = \frac{\lambda}{6} \alpha_0 \bar{a}^3 + \frac{\lambda}{6} \alpha_0 \beta^2 \bar{a} . \tag{2.56}$$

Solution on page 313.

The constant factor in front of the terms in Eq. (2.56) represents the coupling constant g characterizing the strength of the interaction between the fields (or the self-interaction in the case of the $\bar{a}^3$ term). The coupling constant can be re-written in terms of the spontaneous symmetry breaking scale f:

$$g = \frac{\lambda\alpha_0}{6} = \frac{1}{\sqrt{6}}\frac{\mu^2}{f} \sim \frac{\mu^2}{f} \,. \tag{2.57}$$

Accounting for the interaction terms gives a new approximate Lagrangian,

$$\mathcal{L} \approx \frac{1}{2}\left(\partial_\mu \bar{a}\right)^2 + \frac{1}{2}\left(\partial_\mu \beta\right)^2 - \mu^2\bar{a}^2 - 3\epsilon\mu^2\beta^2 + \frac{1}{\sqrt{6}}\frac{\mu^2}{f}\bar{a}^3 + \frac{1}{\sqrt{6}}\frac{\mu^2}{f}\beta^2\bar{a} \,. \tag{2.58}$$

Equations (2.57) and (2.58) highlight another important generic feature of ultralight bosonic fields that makes them good candidates to be dark matter: the coupling to other particles and fields generally scales as $1/f$, so if the symmetry breaking scale is at a very large energy, such as the grand unified theory (GUT) scale ($f \sim 10^{25}$ eV $= 10^{16}$ GeV) or Planck scale ($f \sim 10^{28}$ eV $= 10^{19}$ GeV), nongravitational interactions of the ultralight bosons are strongly suppressed, consistent with astrophysical observations as discussed in Chaps. 1 and 3, and also consistent with the results of the many null experiments described throughout this book.

2.4.1 *Interactions Between Ultralight Bosonic Fields and Standard Model Particles*

If terms describing the Standard Model particles and fields and their interactions are incorporated into the Lagrangian, along with terms describing ultralight bosonic fields, a variety of interaction terms are possible [20]. Many of the couplings studied both in the experiments discussed in this book, as well as in numerous theories of beyond-the-Standard-Model physics, are listed in Table 2.1 (note that the list of couplings is not exhaustive[6]). If dark matter consists primarily of ultralight bosonic fields, these possible nongravitational interactions can be classified into a

[6] The couplings listed in Table 2.1 only include operators up to a certain dimension (see discussion in Ref. [20]). Also, Table 2.1 is compiled assuming a particular basis for the fermions, other bases permit different forms of the couplings. For axions, in particular, it is significant that the fermion interactions generate the other axion interactions via the *chiral anomaly*, called an "anomaly" because it is a case where a classical symmetry of the Lagrangian does not map to a quantum symmetry for the corresponding Lagrangian. In the low temperature limit (where T is well below the QCD phase transition temperature ~200 MeV), the gluon interaction generates the axion mass via soft explicit breaking of the chiral symmetry due to mixing with pions as described in the tutorial at the end of Sect. 2.5.1. In the high temperature limit, the axion mass is generated via

Table 2.1 Couplings of ultralight bosonic fields to Standard Model particles and fields. Examples of ultralight bosons include scalars ϕ, axions (or axionlike particles, ALPs) a, and dark/hidden photons, described by a vector potential $\mathcal{X}_\mu$ and field strength $\mathcal{F}_{\mu\nu}$. Standard Model particles include Higgs bosons h, gluons $G^{\mu\nu}$, photons $F^{\mu\nu}$, and fermions ψ. The dual gluon field tensor is denoted $\tilde{G}^{\mu\nu}$ and the dual electromagnetic tensor is denoted $\tilde{F}^{\mu\nu}$, and A_μ is the photon vector potential. General terms from the Standard Model are denoted by $O_{\rm sm}$. Note that because the Lagrangian is real-valued, the operators must take the appropriate form depending on whether the considered fields are real or complex. The usual Dirac matrices are denoted γ_μ and $\gamma_5 = -i\gamma_0\gamma_1\gamma_2\gamma_3$, and $\sigma^{\mu\nu} = (i/2)[\gamma^\mu, \gamma^\nu]$. The rightmost column list the chapters of the present book in which experiments probing such effects are discussed. Table adapted from Refs. [20] and [24]

Spin	Type	Operator	Interaction	Chapters
0	Scalar	$\phi h^\dagger h$	Higgs portal	8, 10
0	Scalar	$\phi^n O_{\rm sm}$ $(n = 1, 2)$	Dilaton	8, 10
0	Scalar	$\phi^\dagger \partial_\mu \phi \psi^\dagger \gamma^\mu \psi$	Current-current	8, 10
0	Pseudoscalar	$a G^{\mu\nu} \tilde{G}_{\mu\nu}$	Axion-gluon	6
0	Pseudoscalar	$a F^{\mu\nu} \tilde{F}_{\mu\nu}$	Axion-photon	4, 5, 7, 9
0	Pseudoscalar	$(\partial_\mu a)\psi^\dagger \gamma^\mu \gamma_5 \psi$	Axion-fermion	6, 8, 10
1	Vector	$\mathcal{X}_\mu \psi^\dagger \gamma^\mu \psi$	Minimally coupled	8
1	Vector	$F_{\mu\nu}\mathcal{F}^{\mu\nu}$, $A_\mu \mathcal{X}^\mu$	Photon-hidden-photon mixing	7
1	Vector	$\mathcal{F}_{\mu\nu} \psi^\dagger \sigma^{\mu\nu} \psi$	Dipole interaction	6, 8, 10
1	Axial vector	$\mathcal{X}_\mu \psi^\dagger \gamma^\mu \gamma^5 \psi$	Minimally coupled	6, 8, 10

few different phenomenological "portals" between the Standard Model and the dark sector [24], where the portals can be classified by the physical effects the UBDM generates in experiments. In this section, for illustrative purposes, we analyze a few of these different interactions and portals.

Before analyzing particular cases, though, let us consider some general features of the interactions listed in Table 2.1. The first column of Table 2.1 lists the spin of the boson. Here we consider spin-0 (as discussed in Sects. 2.2 and 2.3) and spin-1 bosons, encompassing the majority of presently studied beyond-the-Standard-Model theories.[7] The second column considers the parity symmetry (P) of the interaction. Parity is the symmetry with respect to spatial inversion (reflection of coordinate axes through the origin): under spatial inversion, P-odd quantities change sign (pseudoscalars and vectors) and P-even quantities are invariant (scalars and axial vectors). Parity symmetry is among the key discrete symmetries characterizing interactions, others include time-reversal (T) and charge-

instantons [21, 22]. For further discussion of the chiral anomaly and instantons, see, e.g., Ref. [2]. For the dilaton, the interactions are defined in the Einstein conformal frame [23].

[7] The limitation to bosons with spin ≤ 1 is due in part to the fact that at present there are unresolved theoretical questions concerning the validity, naturalness, and allowed interactions for spin-2 fields with nonzero mass [20]. Presently there is no known effective field theory for bosons with spin ≥ 3 that is valid above the boson mass [20].

conjugation (C).[8] The discrete symmetry properties of an interaction inform the nature of the experiment necessary to observe signatures of particular classes of UBDM candidates.

2.4.2 Axion-Photon Interaction

Let us begin by considering one of the most widely studied UBDM interactions, the axion-photon coupling. The axion-photon coupling is used to convert axions or ALPs into photons in the presence of strong magnetic fields. This is the technique at the heart of the microwave cavity haloscopes described in Chap. 4, the axion helioscopes searching for axion/ALP emission from the Sun described in Chap. 5, axion/ALP searches with "dark matter radios" using lumped-element resonators described in Chap. 7, and light-shining-through-walls experiments discussed in Chap. 9. The fourth row of Table 2.1 describes an operator involving factors of both a spin-0 pseudoscalar axion (ALP) field a and the product of the electromagnetic field tensor (Faraday tensor) $F^{\mu\nu}$ with the dual field tensor $\tilde{F}_{\mu\nu}$. The Faraday tensor $F^{\mu\nu}$ is given by [30]

$$F^{\mu\nu} = \partial^{\mu} A^{\nu} - \partial^{\nu} A^{\mu} \tag{2.59}$$

$$= \begin{pmatrix} 0 & -E_x & -E_y & -E_z \\ E_x & 0 & -B_z & B_y \\ E_y & B_z & 0 & -B_x \\ E_z & -B_y & B_x & 0 \end{pmatrix}, \tag{2.60}$$

where A^{μ} is the four-potential and E_i and B_i are the electric and magnetic field components in the Cartesian basis. The dual field tensor is given by

$$\tilde{F}_{\alpha\beta} = \frac{1}{2} \varepsilon_{\alpha\beta\mu\nu} F^{\mu\nu}, \tag{2.61}$$

where $\varepsilon_{\alpha\beta\mu\nu}$ is the Levi-Civita totally antisymmetric tensor. We note the general structure of the operator for the axion-photon interaction, one factor of the ultralight bosonic field a, and two factors of the photon field. This structure is similar to the interaction terms studied in Problem 2.4, seen perhaps most clearly by writing the operator in terms of the four-potential A^{μ}:

$$a F^{\mu\nu} \tilde{F}_{\mu\nu} = a \epsilon^{\mu\nu\alpha\beta} \left(\partial_{\mu} A_{\nu} \partial_{\alpha} A_{\beta} \right), \tag{2.62}$$

[8] Famously, Wu et al. [25] discovered that the weak interaction violated parity conservation in 1957, and later in 1964 Christenson, Cronin, Fitch, and Turlay [26] discovered violation of the combined CP symmetry. Observations of atomic parity violation [27–29] were crucial in establishing the existence of parity-violating neutral weak currents mediated by the Z-boson.

showing that indeed this term represents an interaction between an axion and two photons.

The term in the Lagrangian describing the axion-photon interaction is

$$\mathcal{L}_{a\gamma\gamma} = \frac{g_\gamma}{4}\frac{\alpha}{\pi}\frac{a}{f_a}F^{\mu\nu}\tilde{F}_{\mu\nu} = \frac{g_{a\gamma\gamma}}{4}aF^{\mu\nu}\tilde{F}_{\mu\nu}\,, \tag{2.63}$$

where g_γ is a dimensionless model-dependent coupling factor, α is the fine structure constant, f_a is the spontaneous symmetry breaking scale for the axion/ALP field, and $g_{a\gamma\gamma} = g_\gamma\alpha/(\pi f_a)$ is the axion-photon coupling constant. Note that the axion-photon coupling is proportional to $1/f_a$, exhibiting the characteristic suppression derived in Eqs. (2.57) and (2.58). The form of the Lagrangian in terms of the electric field $\boldsymbol{E}$ and magnetic field $\boldsymbol{B}$ is

$$\mathcal{L}_{a\gamma\gamma} = g_\gamma\frac{\alpha}{\pi}\frac{a}{f_a}\boldsymbol{E}\cdot\boldsymbol{B} \approx g_{a\gamma\gamma}a\boldsymbol{E}\cdot\boldsymbol{B}\,. \tag{2.64}$$

? Problem 2.5 Axion-Photon Interaction

Derive Eq. (2.64).

Solution on page 314.

In experiments, the magnetic field $\boldsymbol{B}$ appearing in Eq. (2.64) is generated in the laboratory by, for example, current circulating in a superconducting coil, and the electric field $\boldsymbol{E}$ represents the field of the resultant photon generated from the axion. The conversion of axions into photons in a magnetic field is known as the *inverse Primakoff effect* [31–33], illustrated by the Feynman diagram in Fig. 2.7.

One method to calculate the observable physical consequences resulting from the axion-photon interaction is to apply the Euler–Lagrange equation to the Lagrangian describing electromagnetism plus the axion-photon Lagrangian of Eq. (2.63), namely

$$\mathcal{L} = -\frac{1}{4}F^{\mu\nu}F_{\mu\nu} - J^\mu A_\mu + \frac{g_{a\gamma\gamma}}{4}aF^{\mu\nu}\tilde{F}_{\mu\nu}\,, \tag{2.65}$$

where J^μ is the electromagnetic current and A^μ is the gauge potential. The Euler–Lagrange equation in this case produces a version of Maxwell's equations that includes the effects of an axion field, as discussed in Refs. [32–35]:

$$\nabla\cdot\boldsymbol{E} = \rho + g_{a\gamma\gamma}\boldsymbol{B}\cdot\nabla a\,, \tag{2.66}$$

$$\nabla\cdot\boldsymbol{B} = 0\,, \tag{2.67}$$

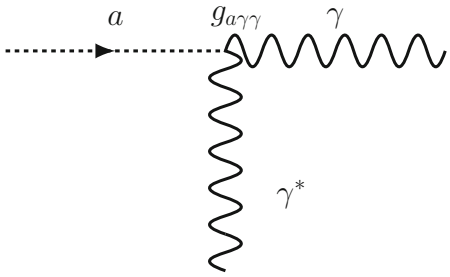

Fig. 2.7 Feynman diagram illustrating the inverse Primakoff effect, where an axion a is converted into a real photon γ by interacting with a virtual photon γ^* sourced by a magnetic field (a virtual photon is one that does not need to satisfy the energy-momentum relationship or "on-shell" dispersion equation, see discussion in Refs. [1–5]). The axion-photon interaction is parameterized by the axion-photon coupling constant $g_{a\gamma\gamma}$, see Eqs. (2.63) and (2.64)

$$\nabla \times \boldsymbol{E} = -\frac{\partial \boldsymbol{B}}{\partial t} \,, \tag{2.68}$$

$$\nabla \times \boldsymbol{B} = \frac{\partial \boldsymbol{E}}{\partial t} + \boldsymbol{J} + g_{a\gamma\gamma}\left(\boldsymbol{E} \times \nabla a - \frac{\partial a}{\partial t}\boldsymbol{B}\right) , \tag{2.69}$$

where ρ is the charge density and $\boldsymbol{J}$ is the electric current density.

Physical observables that can be searched for in experiments can be derived from these modified Maxwell's equations. (A similar approach for understanding hidden photon experiments is described in detail in Chap. 7.) Consider, for example, a region of vacuum ($\rho = 0$ and $\boldsymbol{J} = 0$) bounded by a perfect conductor in the shape of an infinite cylinder with radius R. Inside this cylindrical region, a magnetic field $\boldsymbol{B}_0$ is applied along the cylinder axis ($\hat{\boldsymbol{z}}$), such that $\boldsymbol{B} = B_0 \boldsymbol{z}$ for $r \leq R$ and $\boldsymbol{B} = 0$ for $r > R$. Further, let us assume that the Compton wavelength of the axion (equal to $1/m_a$ in natural units, where m_a is the axion mass) is large compared to the cylinder dimensions, $m_a R \ll 1$. This is the case for "dark matter radio" experiments (discussed in Chap. 7) that search for UBDM candidates whose Compton wavelengths are so large that construction of resonant cavities is impractical. In such cases the axion de Broglie wavelength is also large compared to the cylinder dimensions, meaning that the spatial gradient of the axion field can be neglected in this treatment ($\nabla a \approx 0$). To analyze this system, we differentiate between the total magnetic field $\boldsymbol{B}$ and the induced fields $\mathcal{E}$ and $\mathcal{B}$ from the axion-photon interaction, such that $\boldsymbol{B} = \boldsymbol{B}_0 + \mathcal{B}$. With these assumptions, noting that $\boldsymbol{B}_0 \gg \mathcal{B}$, the modified Maxwell's equations become

$$\nabla \cdot \mathcal{E} = 0 \,, \tag{2.70}$$

$$\nabla \cdot \mathcal{B} = 0 \,, \tag{2.71}$$

$$\boldsymbol{\nabla} \times \mathcal{E} = -\frac{\partial \mathcal{B}}{\partial t} \,, \tag{2.72}$$

$$\boldsymbol{\nabla} \times \mathcal{B} = \frac{\partial \mathcal{E}}{\partial t} - g_{a\gamma\gamma} \frac{\partial a}{\partial t} \boldsymbol{B}_0 \,. \tag{2.73}$$

Taking the curl of Eq. (2.73), and making use of the identity

$$\boldsymbol{\nabla} \times (\boldsymbol{\nabla} \times \mathcal{B}) = \boldsymbol{\nabla}(\boldsymbol{\nabla} \cdot \mathcal{B}) - \nabla^2 \mathcal{B} \,, \tag{2.74}$$

as well as Eqs. (2.71) and (2.72), we find

$$-\nabla^2 \mathcal{B} = \frac{\partial}{\partial t}\left(-\frac{\partial \mathcal{B}}{\partial t}\right) - g_{a\gamma\gamma} \frac{\partial a}{\partial t} (\boldsymbol{\nabla} \times \boldsymbol{B}_0) = -\frac{\partial^2 \mathcal{B}}{\partial t^2} \,, \tag{2.75}$$

where we used the fact that $\boldsymbol{\nabla} \times \boldsymbol{B}_0 = 0$. A similar approach yields

$$-\nabla^2 \mathcal{E} = -\frac{\partial^2 \mathcal{E}}{\partial t^2} + g_{a\gamma\gamma} \frac{\partial^2 a}{\partial t^2} \boldsymbol{B}_0 \,, \tag{2.76}$$

and so we arrive at the wave equations

$$\nabla^2 \mathcal{B} - \frac{\partial^2 \mathcal{B}}{\partial t^2} = 0 \,, \tag{2.77}$$

$$\nabla^2 \mathcal{E} - \frac{\partial^2 \mathcal{E}}{\partial t^2} = -g_{a\gamma\gamma} \frac{\partial^2 a}{\partial t^2} \boldsymbol{B}_0 \,. \tag{2.78}$$

As discussed in Sect. 2.2, if axions are the dark matter, they are nonrelativistic and thus manifest as a field oscillating at the Compton frequency m_a. As noted in Chap. 1, the axion field has a relatively long coherence time, so a good initial model for the axion field is

$$a(\boldsymbol{r}, t) = a_0 e^{i(\boldsymbol{k}\cdot\boldsymbol{r} - m_a t)} \,, \tag{2.79}$$

where $\boldsymbol{k}$ is the wave vector. Taking into account the cylindrical symmetry of the cavity and the boundary condition that the electric field parallel to the conducting surface at $r = R$ is zero, the wave equations (2.77) and (2.78) are solved by

$$\mathcal{E}(\boldsymbol{r}, t) = g_{a\gamma\gamma} a_0 e^{-i m_a t} \boldsymbol{B}_0 \left(1 - \frac{J_0(m_a r)}{J_0(m_a R)}\right) , \tag{2.80}$$

$$\mathcal{B}(\boldsymbol{r}, t) = i g_{a\gamma\gamma} a_0 e^{-i m_a t} B_0 \hat{\boldsymbol{\phi}} \left(\frac{J_1(m_a r)}{J_1(m_a R)}\right) , \tag{2.81}$$

where $J_n(x)$ is the is the nth order Bessel function of the first kind [36, 37], and where we have used the fact that $e^{i\boldsymbol{k}\cdot\boldsymbol{r}} \approx 1$. For $m_a r \leq m_a R \ll 1$, the Bessel

functions can be approximated by the lowest order terms in their Taylor expansion, and so

$$\mathcal{E}(\boldsymbol{r}, t) \approx g_{a\gamma\gamma} a_0 e^{-im_a t} \boldsymbol{B}_0 \left(m_a^2 R^2 - m_a^2 r^2 \right) , \tag{2.82}$$

$$\mathcal{B}(\boldsymbol{r}, t) \approx i g_{a\gamma\gamma} a_0 e^{-im_a t} B_0 \hat{\boldsymbol{\phi}}(m_a r) . \tag{2.83}$$

Note that in this case, the magnitude of the induced electric field is suppressed compared to that of the magnetic field by a factor of $\approx m_a R \ll 1$.

Based on the above analysis, it is evident that the axion field is a source term that can, in principle, generate measurable electromagnetic energy via the inverse Primakoff effect. Experiments searching for axion and ALP dark matter using the axion-photon coupling are discussed in detail in Chaps. 4, 5, and 9, and the closely related case of dark matter radio searches for hidden photons is discussed in Chap. 7.

2.4.3 Axion-Fermion Interaction

A number of experiments search for couplings between axions/ALPs and fermions, for example, the Cosmic Axion Spin Precession Experiment (CASPEr, see Ref. [38]) and the QUest for AXions experiment (QUAX, see Ref. [39]) discussed in Chap. 6 and the Global Network of Optical Magnetometers to search for Exotic physics (GNOME, see Refs. [40, 41]) described in Chap. 10, as well as experiments searching for long-range interactions between fermions mediated by axions or ALPs (such as the Axion Resonant InterAction Detection Experiment, ARIADNE, see Ref. [42]), discussed in Chap. 8.

One possible axion-fermion interaction is described by the Lagrangian term

$$\mathcal{L}_{a\mathrm{ff}} = \frac{g_\mathrm{f}}{f_a} \left(\partial_\mu a \right) \psi^\dagger \gamma^\mu \gamma_5 \psi , \tag{2.84}$$

where g_f is a dimensionless model-dependent coupling factor and $\psi^\dagger \gamma^\mu \gamma_5 \psi$ is the axial-vector current for a Standard Model fermion f. The Hamiltonian $\mathcal{H}_{a\mathrm{f}}$ describing this interaction can be calculated from the Euler–Lagrange equations according to

$$\mathcal{H}_{a\mathrm{f}} \psi = -\gamma_0 \left[\frac{\partial \mathcal{L}_{a\mathrm{ff}}}{\partial \psi^\dagger} - \partial_\mu \left(\frac{\partial \mathcal{L}_{a\mathrm{ff}}}{\partial \left(\partial_\mu \psi^\dagger \right)} \right) \right] , \tag{2.85}$$

$$= -\frac{g_\mathrm{f}}{f_a} \gamma_0 \gamma^\mu \gamma_5 \psi \left(\partial_\mu a \right) . \tag{2.86}$$

The Dirac matrices can be evaluated according to

$$\gamma_0\gamma^\mu\gamma_5 = (\gamma_0\gamma_0\gamma_5, -\gamma_0\gamma_1\gamma_5, -\gamma_0\gamma_2\gamma_5, -\gamma_0\gamma_3\gamma_5)\ , \tag{2.87}$$

$$= (\gamma_5, -\Sigma_1, -\Sigma_2, -\Sigma_3)\ , \tag{2.88}$$

$$= (\gamma_5, -\boldsymbol{\Sigma})\ , \tag{2.89}$$

where the parentheses enclose a list of the individual components of $\gamma_0\gamma^\mu\gamma_5$, evident from the definition $\gamma^\mu = (\gamma_0, \gamma_1, \gamma_2, \gamma_3)$, and where

$$\boldsymbol{\Sigma} = \begin{pmatrix} \boldsymbol{\sigma} & 0 \\ 0 & \boldsymbol{\sigma} \end{pmatrix}\ , \tag{2.90}$$

with $\boldsymbol{\sigma}$ being the Pauli spin matrices, and where we have employed the identities

$$\gamma_0\gamma_0 = 1 \tag{2.91}$$

and

$$\gamma_0\gamma_i\gamma_5 = \Sigma_i\ . \tag{2.92}$$

Thus the Hamiltonian $\mathcal{H}_{af}$ appearing in Eq. (2.86) can be written as

$$\mathcal{H}_{af}\psi = -\frac{g_f}{f_a}(\gamma_5, -\boldsymbol{\Sigma})\psi\,\partial_\mu a\ , \tag{2.93}$$

$$= -\frac{g_f}{f_a}\left(\gamma_5\psi\frac{\partial a}{\partial t} + (\boldsymbol{\Sigma}\psi)\cdot\boldsymbol{\nabla}a\right)\ , \tag{2.94}$$

and taking the nonrelativistic limit, in which the spacelike component is much larger than the time-like component, Eq. (2.94) becomes

$$\mathcal{H}_{af} \approx -\frac{g_f}{f_a}\frac{\boldsymbol{S}}{|S|}\cdot\boldsymbol{\nabla}a\ , \tag{2.95}$$

where $\boldsymbol{S}$ is the fermion spin and $|S|$ is the spin magnitude. It is important to note that not only does $\mathcal{H}_{af}$ generate an interaction between spins and the spatial gradient of the axion field but also an interaction between spins who are moving with respect to an axion field, since the momentum operator $\boldsymbol{p} = -i\boldsymbol{\nabla}$. This effect is known as the "axion wind" interaction and is a consequence of the fact that the field gradient is frame-dependent. The axion gradient interaction (encompassing the effects of spatial gradients and the wind interaction) is searched for in experiments such as CASPEr (the Cosmic Axion Spin Precession Experiment [43–45]) and GNOME (the Global Network of Optical Magnetometers for Exotic physics searches [40, 41, 46]) as discussed in Chaps. 6 and 10, respectively.

2.5 Theoretical Motivations for Ultralight Bosons

As noted in Chap. 1, theoretically well-motivated dark matter candidates have additional hints of their existence beyond just the evidence for dark matter. In other words, well-motivated dark matter candidates also solve other mysteries of physics. One of the most prominent examples of such a UBDM candidate is the axion, which originally emerged from an elegant solution to the strong CP problem [47, 48], the mystery of why CP-violating nuclear electric dipole moments are many orders of magnitude smaller than nominally predicted by quantum chromodynamics (QCD). As a consequence this particular ultralight boson is known as the *QCD axion*. A variety of other theories have emerged predicting similar axionlike particles (ALPs) [19]. One example such is the *relaxion*, proposed to solve the hierarchy problem [49], the question of why the Higgs boson mass is so much lighter than the Planck mass (or, in other words, why the electroweak interaction so much stronger than gravity). Axions and ALPs also offer a mechanism to explain the asymmetry between matter and antimatter in the universe [50, 51]. Attempts to unify general relativity and quantum field theory, such as string theories, generically predict the existence of axions, ALPs and other spin-0 bosons [52, 53] as well as spin-1 bosons such as dark or hidden photons [54, 55]. The key takeaway is that ultralight bosons are well-motivated from a wide variety of theoretical perspectives. In this section we explore the basic ideas behind some illustrative examples of ultralight bosons, the QCD axion, the relaxion, and axions arising from the extra dimensions appearing in string theory.

2.5.1 Peccei-Quinn Solution to the Strong C P Problem and the QCD Axion

The QCD axion is a natural consequence of the solution to the strong CP problem first proposed by Peccei and Quinn [47, 48, 56, 57]. The strong CP problem is related to the non-observation of a permanent electric dipole moment (EDM) of the neutron [58] and various nuclei [59] (such as ^{199}Hg, which gives the best constraint at present [60]). The magnitude of the neutron EDM d_n is predicted by the Standard Model to be [61–64]

$$|d_n| \sim 10^{-16} \bar{\theta}_{\rm QCD}\ e \cdot {\rm cm}\ , \tag{2.96}$$

where $\bar{\theta}_{\rm QCD}$ is a CP-violating parameter appearing in the Lagrangian for the strong interaction. $\bar{\theta}_{\rm QCD}$ is a phase angle that, in principle, can take on any value, so, based on "naturalness" its value (modulo 2π) should nominally be $\bar{\theta}_{\rm QCD} \sim 1$. Thus the Standard Model nominally predicts a neutron EDM of $|d_n| \sim 10^{-16}\ e{\cdot}$cm. However, the current experimental limit on the neutron EDM is [58]

$$|d_n| < 1.8 \times 10^{-26}\ e \cdot {\rm cm}\ , \tag{2.97}$$

which leads to the conclusion that $\left|\bar{\theta}_{\rm QCD}\right| \lesssim 2 \times 10^{-10}$ (the ^{199}Hg EDM constraint [60] suggests a similar limit [65, 66]). One may wonder if $\bar{\theta}_{\rm QCD}$ is simply a very small number by accident. However, the observable $\bar{\theta}_{\rm QCD}$ actually arises from two contributions to the Standard Model. For these two contributions to cancel with such precision would be unnatural.

The first of these contributions is the θ parameter, which appears in a term in the QCD Lagrangian:

$$\mathcal{L}_\theta = \theta \frac{\alpha_s}{8\pi} G^{(a)}_{\mu\nu} \tilde{G}^{(a)\mu\nu} \,, \tag{2.98}$$

where $\alpha_s \sim 1$ is the coupling constant for the gluon field, $G^{(a)}_{\mu\nu}$ is the gluon field strength tensor (where $a = 1, 2, \ldots, 8$ indicate the eight gluon color charges), and $\tilde{G}^{(a)\mu\nu} = (1/2)\varepsilon^{\mu\nu\alpha\beta} G^{(a)}_{\alpha\beta}$ is the dual gluon field strength tensor (the gluon field strength tensor is analogous to the Faraday tensor for electromagnetism, see, for example, Refs. [2, 3]). Note that $G^{(a)}_{\mu\nu}\tilde{G}^{(a)\mu\nu}$ violates CP symmetry, just as $F^{\mu\nu}\tilde{F}_{\mu\nu} \propto \boldsymbol{E} \cdot \boldsymbol{B}$ does for electromagnetism (as seen from the fact that $\boldsymbol{E} \cdot \boldsymbol{B}$ is P- and T-odd). The θ parameter is associated with the QCD vacuum state $|\theta\rangle$ parametrized by the angle $0 \leq \theta < 2\pi$ (see Refs. [14, 16] for further discussion). However, it turns out that the angle θ is not invariant with respect to *chiral transformation* (i.e., parity transformation or helicity exchange) for nonzero quark masses.

While in the limit of massless quarks, QCD would possess a chiral symmetry, such a symmetry is broken by the Adler-Bell-Jackiw anomaly [67, 68] if the quark masses are nonzero. For massive quarks, QCD physics is invariant under the following transformation of the quark fields and masses, q_i and m_i, respectively, and the vacuum parameter θ:

$$q_i \to e^{i\alpha_i \gamma_5/2} \,, \tag{2.99}$$

$$m_i \to e^{-i\alpha_i} m_i \,, \tag{2.100}$$

$$\theta \to \theta - \sum_{i=1}^{N} \alpha_i \,, \tag{2.101}$$

where α_i are the phases of the N quark fields.[9] While θ is thus not an invariant of QCD, the combination

$$\bar{\theta}_{\rm QCD} \equiv \theta - \arg\left(\det \mathcal{M}_q\right) = \theta - \arg\left(\prod_{i=1}^{N} m_i\right) \tag{2.102}$$

[9] Note that Eq. (2.101), a rotation of the fermion determinant, is highly nontrivial: for more detailed discussion see Refs. [14–17] and for a pedagogical treatment see Ref. [5].

is invariant and thus observable ($\mathcal{M}_q$ is the quark mass matrix, see Refs. [2, 69] for definition and discussion). The strong CP problem is the question of why $\bar{\theta}_{\rm QCD}$ is so small. Given that θ describes the QCD vacuum and that quark masses are due to the Higgs mechanism, a naive estimate for such a phase parameter is that it is of order one. Therefore the observed exceedingly small $\bar{\theta}_{\rm QCD}$ is unnatural.

The Peccei-Quinn solution to the strong CP problem allows $\bar{\theta}_{\rm QCD}$ to be small in a natural way, by promoting it to a dynamical variable that naturally relaxes to zero, at the minimum of a potential. To do this, the Standard Model must be extended with the introduction of additional degrees of freedom, while preserving the existing symmetries of the Standard Model. To achieve this, Peccei and Quinn [47, 48] introduced a global, chiral $\mathbb{U}(1)$ symmetry, now known as the Peccei-Quinn (PQ) symmetry, $\mathbb{U}(1)_{PQ}$ (see the tutorial at the end of Sect. 2.3 involving the $\mathbb{U}(1)$ symmetry). This symmetry is spontaneously broken at some scale, f_a, a parameter of the model, and the resulting pseudo-Nambu-Goldstone boson is the axion.

The way in which the required additional degree of freedom is introduced is model-dependent. Peccei and Quinn originally tied the symmetry breaking scale to the electroweak scale, but this resulted in an axion with a mass and couplings that would have been observed in experiments, and thus this original axion model was rapidly ruled out. Other axion models were quickly proposed that resulted in a much lighter axion with small couplings to Standard Model particles. The nature of these couplings made these axions difficult to detect, and thus they are sometimes called "invisible" axion models.

Here, we will review the Peccei-Quinn-Weinberg-Wilczek (PQWW) axion model [47, 48, 56, 57]. The original Peccei-Quinn proposal was implemented using two Higgs doublets h_u and h_d, which, respectively, couple to the up-type quarks with isospin $+1/2$, and the down-type quarks with isospin $-1/2$. The quark masses are then generated from the following Yukawa couplings to the neutral components of the Higgs fields

$$\mathcal{L}_m = y_i^u u_{Li}^\dagger h_u^0 u_{Ri} + y_i^d d_{Li}^\dagger h_d^0 d_{Ri} + \text{h.c.}, \tag{2.103}$$

where for N total quarks, there are $N/2$ up-type quarks, u_i, and $N/2$ down-type quarks, d_i, subscripts L and R denote left and right quark chirality, respectively, and the y_i are the Yukawa couplings to the quark type denoted by the superscript. Peccei and Quinn chose the Higgs potential to be

$$V(h_u, h_d) = -\mu_u^2 h_u^\dagger h_u + \mu_d^2 h_d^\dagger h_d + \sum_{i,j} \left(A_{ij} h_i^\dagger h_i h_j^\dagger h_j + B_{ij} h_i^\dagger h_j h_j^\dagger h_i \right), \tag{2.104}$$

where the coefficient matrices (A_{ij}) and (B_{ij}) are real and symmetric, and the sum is over the two types of Higgs fields. The $\mathbb{U}_{PQ}(1)$ invariance is manifested as the Lagrangian, $\mathcal{L} \equiv \mathcal{L}_m + V$, is invariant under the following transformations:

$$u_i \to e^{-i\alpha_u \gamma_5} u_i \tag{2.105}$$

$$d_i \rightarrow e^{-i\alpha_d \gamma_5} d_i \tag{2.106}$$

$$h_u \rightarrow e^{i2\alpha_u} h_u \tag{2.107}$$

$$h_d \rightarrow e^{i2\alpha_d} h_d \ . \tag{2.108}$$

Under the transformations (2.105)–(2.108), by applying Eqs. (2.101) and (2.102) one finds that $\bar{\theta}_{\rm QCD}$ is also transformed according to

$$\bar{\theta}_{\rm QCD} \rightarrow \bar{\theta}_{\rm QCD} - N(\alpha_u + \alpha_d) \ . \tag{2.109}$$

In this model, when the Universe cools to the electroweak symmetry breaking scale, the neutral Higgs acquire vacuum expectation values,

$$\langle h_u^0 \rangle = v_u e^{i P_u / v_u} \tag{2.110}$$

$$\langle h_d^0 \rangle = v_d e^{i P_d / v_d} \ , \tag{2.111}$$

where P_u and P_d are the Nambu-Goldstone fields. One linear combination of these fields becomes the longitudinal component of the Z-boson, $\mathcal{Z}$, as per standard electroweak symmetry breaking, and the other combination is the axion field, a:

$$\mathcal{Z} = P_u \cos\beta_v - P_d \sin\beta_v \tag{2.112}$$

$$a = P_u \sin\beta_v + P_d \cos\beta_v \ . \tag{2.113}$$

Using Eqs. (2.110) through (2.113) gives the following for the quark masses in Eq. (2.103):

$$-\mathcal{L}_m = m_i^u u_{Li}^\dagger e^{(i \sin\beta_v / v_u) a} u_{Ri} + m_i^d d_{Li}^\dagger e^{(i \cos\beta_v / v_d) a} d_{Ri} + \text{ h.c. } , \tag{2.114}$$

where the quark masses are $m_i^u = y^{u_i} v_u$ and $m_i^d = y_i^d v_d$.

Using the quark transformations of Eqs. (2.105) and (2.106) with Eq. (2.109), the axion dependence can be removed from the quark mass terms. The change in $\bar{\theta}_{\rm QCD}$ due to the transformation of Eq. (2.109) can be absorbed by a redefinition of the axion field. This end result is that the $\bar{\theta}_{\rm QCD}$ parameter of QCD is replaced by the axion field a. That is, a static parameter required to have a single value, which is not necessarily small, is replaced by a dynamical field. When given a potential, this dynamical field will relax to the minimum of the potential, providing a natural explanation for CP conservation in the Standard Model.

Tutorial: Mass of the QCD Axion

The axion mass, m_a, depends on the value of the axion decay constant, f_a, via

$$m_a \simeq 6 \times 10^{-6}\ \text{eV} \left(\frac{10^{12}\ \text{GeV}}{f_a} \right) . \tag{2.115}$$

This was first derived using the methods of current algebra by Weinberg [56], and by Bardeen and Tye [70], although Bardeen and Tye used the name "higglet" for the axion at this early stage of its study. Note that as in Eq. (2.45), the mass of the axion is $\propto 1/f_a$.

The axion mass can be determined by considering the chiral effective Lagrangian at low energies for axions and pions. This may be written as

$$\begin{aligned} \mathcal{L}_{\pi a} = & \frac{1}{2} \partial_\mu a' \partial^\mu a' + \frac{f_\pi^2}{4} \text{Tr}\Big[\partial_\mu U^\dagger(\boldsymbol{\pi}) \partial^\mu U(\boldsymbol{\pi}) \Big] \\ & + \Lambda_{\text{QCD}}^3 \text{Tr}\Big[\mathcal{M}_q U(\boldsymbol{\pi}) e^{-ia'/(2f_a)} + \text{h.c.} \Big] , \end{aligned} \tag{2.116}$$

where $\Lambda_{\text{QCD}} \sim 200$ MeV is the QCD confinement scale (which gives rise to the explicit symmetry breaking for the QCD axion, and is thus roughly equivalent to the Λ discussed in Sect. 2.3), the pion triplet is represented by the field $\boldsymbol{\pi}$, and

$$U(\boldsymbol{\pi}) = \exp\left(\frac{i \boldsymbol{\pi} \cdot \boldsymbol{\sigma}}{f_\pi} \right) , \tag{2.117}$$

with f_π as the pion decay constant, 93 MeV, and $\boldsymbol{\sigma}$ are the Pauli matrices. The third term in Eq. (2.116) describes the explicit breaking of chiral symmetry for pions and axions and works in much the same way as the breaking of the $\mathbb{U}(1)$ symmetry discussed in the tutorial at the end of Sect. 2.3 and illustrated in Fig. 2.6. Therefore Λ_{QCD} plays a role analogous to the Λ discussed in Sect. 2.3. The origin of this symmetry breaking term is discussed in further detail in Refs. [71, 72] and can also be understood in analogy with the theory of antiferromagnetism [12].

The physical axion and neutral pion fields can be evaluated by expanding around the minimum of the potential arising from explicit symmetry breaking, assuming two light quarks [56, 71, 72], to give

$$\pi^0_{\text{phys}} = \pi^0 + \frac{m_d - m_u}{m_d + m_u} \frac{f_\pi}{2 f_a} a' + \mathcal{O}\left(\frac{f_\pi^2}{f_a^2} \right) \tag{2.118}$$

$$a_{\text{phys}} = a' - \frac{m_d - m_u}{m_d + m_u} \frac{f_\pi}{2 f_a} \pi^0 + \mathcal{O}\left(\frac{f_\pi^2}{f_a^2} \right) , \tag{2.119}$$

and the corresponding masses for these fields are then

$$m_{\pi^0}^2 = \Lambda_{\text{QCD}}^3 \frac{m_u + m_d}{f_\pi^2} + \mathcal{O}\left(\frac{f_\pi^2}{f_a^2} \right) \tag{2.120}$$

$$m_a^2 = \Lambda_{\rm QCD}^3 \frac{m_u m_d}{f_a^2 (m_u + m_d)} + O\left(\frac{f_\pi^2}{f_a^2}\right) \tag{2.121}$$

$$\approx \frac{f_\pi^2 m_\pi^2}{f_a^2} \frac{m_u m_d}{(m_u + m_d)^2} \,. \tag{2.122}$$

With the accepted values of m_π, f_π, m_u, and m_d, the axion mass is as given in Eq. (2.115).

This tutorial computed the axion mass using *chiral perturbation theory* in QCD, which is valid for temperatures far below the QCD phase transition (technically, a cross over), $T \ll \Lambda_{\rm QCD} \approx 200$ MeV. At high temperatures, the axion mass becomes temperature dependent, i.e., $m_a = m_a(T)$. The temperature dependence can be estimated using the so-called instanton methods, where the canonical "dilute instanton gas approximation" leads to [73, 74]:

$$m_a \propto T^{-4} \,. \tag{2.123}$$

Non-perturbative lattice QCD methods can interpolate through the QCD phase transition between the two regimes, see Ref. [75]. As we will see, the temperature dependence of the axion mass plays an important role in determining the UBDM relic density in this model.

The power of temperature in the relation Eq. (2.123) depends on the particle content of the Standard Model. The power T^{-4} is valid in a limited regime, and changes at higher temperatures where there are more effectively massless particles. A generic ALP does not obtain its mass from QCD. If the ALP mass comes, for example, from a strongly coupled "hidden sector" based on, but not equivalent to, the Standard Model, then the temperature dependence can be found via methods described in, for example, Ref. [76].

End of Tutorial

2.5.2 The Hierarchy Problem and the Relaxion

One of the greatest mysteries of theoretical physics is the hierarchy problem: why is gravity is so much weaker than all other forces? At the heart of this problem is the question of why the observed Higgs mass ($m_h \approx 125$ GeV) is so much lighter than the Planck mass ($M_{\rm Pl} \sim 10^{19}$ GeV), for one would expect that quantum corrections would cause the effective Higgs mass to be closer to the Planck scale [77–79]. Attempts to solve the hierarchy problem include, for example, supersymmetry [80] and large (sub-mm) extra dimensions [81, 82]. Graham et al. [49] propose that instead the hierarchy problem can be solved by dynamic relaxation of the effective Higgs mass from the Planck scale to the electroweak scale in the early universe.

The dynamics are driven by inflation and a coupling of the Higgs boson to a spin-0 particle dubbed the relaxion. The relaxion could, in principle, be the QCD axion or an ALP [49] and could also constitute the dark matter [83–85]. (although it should be noted that there are issues with fine-tuning in some models [86].)

The basic idea is that inflation in the early universe causes the relaxion field to evolve in time, and because of the coupling between the relaxion and the Higgs, the effective Higgs mass evolves as well. The coupling between the relaxion and the Higgs generates a periodic potential for the relaxion once the Higgs' vacuum expectation value (VEV) becomes nonzero. When the periodic potential barriers become large enough, the time evolution of the relaxion halts and the effective mass of the Higgs settles at its observed value. The electroweak symmetry breaking scale is a special point in the evolution of the Higgs mass. This explains why the Higgs mass eventually settles at the observed value: relatively close to the electroweak scale and far from the Planck scale.

Following the discussion of Refs. [49, 87], let us suppose that the dynamics of the Higgs h and a relaxion φ are governed by a potential of the form

$$V_r(\varphi, h) = \Lambda^3 g\varphi - \frac{1}{2}\Big(\Lambda^2 - g\Lambda\varphi\Big)|h|^2 + \epsilon\Lambda_c^3 h\cos(\varphi/f)\ , \tag{2.124}$$

where Λ is the "ultraviolet cutoff" of the effective field theory (the energy scale beyond which the theory is no longer valid), g is a coupling parameter, Λ_c is the energy scale at which soft explicit symmetry breaking for the relaxion occurs ($\Lambda_c \sim \Lambda_{\rm QCD}$ for the QCD axion), and f is the spontaneous symmetry breaking scale for the relaxion. The first term in Eq. (2.124), $\Lambda^3 g\varphi$, is the leading order term of a Taylor expansion of the relaxion potential arising due to the g-coupling. The second term in Eq. (2.124) gives the effective mass m_h of the Higgs since it is of the form $m_h^2|h|^2/2$ [see, for example, the discussion surrounding Eq. (2.13)], so

$$m_h^2 \approx g\Lambda\varphi - \Lambda^2\ . \tag{2.125}$$

The third term in Eq. (2.124), $\epsilon\Lambda_c^3 h\cos(\varphi/f)$, describes the periodic potential for the relaxion arising from explicit symmetry breaking (for example, due to QCD effects). A sketch of the potential $V_r(\varphi, h)$ is shown in Fig. 2.8.

Now suppose that in the very early universe during inflation, the relaxion field starts with a large value, $\varphi \gtrsim \Lambda/g$ (indicated by the rightmost faded red dot in Fig. 2.8). It is energetically favorable for φ to decrease, and so, under certain conditions, the relaxion field will "slowly roll" down the potential (as indicated by the dashed green arrow and subsequent less faded red dots appearing to the left in Fig. 2.8). The rolling can be slow due to *Hubble friction*, which arises from the term $3H(t)\partial\varphi/\partial t$ appearing in the equation of motion for a scalar field in an expanding universe, where $H(t)$ is the Hubble parameter (as discussed in Sect. 2.6.1). As long as the Hubble friction is sufficiently large so that the dynamics are in the overdamped regime, then φ reaches a "terminal velocity" and the dynamics are independent of the initial conditions. When the evolution of φ reaches the critical

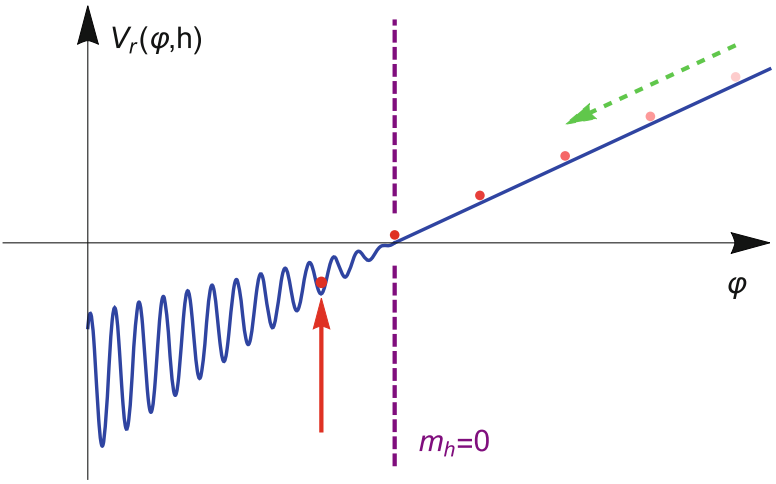

Fig. 2.8 Plot of the relaxion potential $V_r(\varphi, h)$ and illustration of the dynamics. The relaxion field φ starts at a relatively large value (shown by the faded red dots) and then "slowly rolls" down the potential (as indicated by the green dashed arrow), decreasing in amplitude, which in turn decreases m_h according to Eq. (2.125). When the Higgs' vacuum expectation value becomes nonzero at the onset of spontaneous symmetry breaking at $m_h = 0$ (marked by the dashed purple line), the amplitude of the periodic potential for φ increases. Shortly after spontaneous symmetry breaking occurs the potential wells become too deep and φ becomes trapped in a local minimum (shown by the leftmost red dot marked by the red arrow), which sets the scale of m_h at a value $\ll \Lambda$, far from the Planck scale

point $\varphi = \Lambda/g$ where $m_h = 0$, spontaneous symmetry breaking occurs (via mechanisms analogous to those discussed in Sect. 2.3), and the Higgs develops a nonzero vacuum expectation value $\langle h \rangle$. As φ decreases further, $\langle h \rangle$ grows and the amplitude of the periodic potential for φ grows as well. When the periodic potential barriers become sufficiently large, the relaxion will settle into a local minimum (as indicated by the leftmost red dot marked with a red arrow in Fig. 2.8). Again the "slow rolling" condition caused by Hubble friction is important to trap φ in the local minimum.

The crucial point is that the local minimum where φ settles is close to where $m_h \approx 0$, far from Λ and the Planck scale, thereby offering a possible dynamical solution to the hierarchy problem.

2.5.3 UBDM from Extra Dimensions

String theory [88] provides a ubiquitous font of inspiration for new and exotic physics, and the case of UBDM scenarios is no exception. String theory dictates that physics takes place not in the usual four dimensions of spacetime, but in ten. In general relativity (GR) the geometry of the extra dimensions of spacetime should be

described by new functions in the metric tensor, which themselves depend on space and time. Furthermore, the curvature of space itself gravitates and carries energy. The extra dimensions of spacetime in string theory must be small enough such that we have not noticed them. However, since the curvature of these extra dimensions can change from place to place, we might feel the gravitational influence of these changes. This is one way in which string theory realizes UBDM, giving rise to scalar *moduli* and pseudoscalar *axions*.

Let us look at a simple example, which occurs in string theory, but also in any theory with extra spacetime dimensions (such as Kaluza–Klein theory [89, 90], Randall–Sundrum theory [91, 92], and various higher dimensional supergravity theories [93]). Consider the case with spacetime being D-dimensional, given by (3+1) dimensional flat Minkowski space (the manifold $\mathcal{M}_4$), with coordinates $t, \boldsymbol{x}$, and one extra compact dimension (the manifold $\mathcal{S}^1$, topologically the circle), with coordinate θ around it. In GR, this is specified by the metric:

$$ds^2 = -dt^2 + d\boldsymbol{x}^2 + \rho(\boldsymbol{x}, \theta, t)^2 L^2 d\theta^2 \,. \tag{2.126}$$

The dimensionless scalar function ρ specifies how the radius of the "circle" varies compared to a reference length scale L (the typical size of the extra dimension, which should be small). ρ can vary along the circle's circumference as θ changes, and is also a function of space and time in "our" dimensions of Minkowski space. The field ρ is known as the *radion*. Such a situation is possible to picture if we imagine that space is a single dimension like a tightrope, and ρ describes how the cross section of the tight rope varies along its length. If we walk along the tightrope, we cannot see the change in ρ, but a small creature like an ant could, by circling the rope. We may, however, indirectly notice a change in the thickness of the rope, its texture, or some other property.

General relativity tells us that the physics of the theory described by Eq. (2.126) is determined by the Einstein–Hilbert action:

$$S = \frac{M_D^{D-2}}{2} \int dt d^3x L d\theta \sqrt{-g_D} \mathcal{R}_D \,, \tag{2.127}$$

where D is the total number of spacetime dimensions, M_D is the D-dimensional reduced Planck mass, g_D is the D-dimensional metric determinant, and $\mathcal{R}_D$ is the D-dimensional Ricci scalar.

Without going into the details, all we need to know is that the Ricci scalar is a function which is second order in derivatives of the metric components, in this case ρ. The θ dependence of ρ can be found by expanding in terms of the eigenfunctions of $\mathcal{S}^1$, in this case leading simply to a Fourier series:

$$\rho(\boldsymbol{x}, \theta, t) = \sum_n \rho_n(\boldsymbol{x}, t) \cos(n\theta) \,. \tag{2.128}$$

The components ρ_n are four dimensional scalars known as the Kaluza–Klein "tower." It is now possible, if a little cumbersome, to analytically perform the integral $d\theta$ in Eq. (2.127), leaving an action that is second order in derivatives of the scalar fields ρ_n. This process of doing the integral over the compact coordinates, in this case θ, goes under the fancy name of "dimensional reduction"—but it is simply an integral of a series expansion.

A little thought should convince you that derivatives with respect to θ in the Ricci scalar pull down powers of n for $n > 0$. Thus the modes in the tower with $n > 0$ have terms in the action like $(n^2/L^2)\rho_n^2$: this looks like a mass term for ρ_n, which is large if L is small. Thus, for low energy physics we typically neglect the higher modes in the Kaluza–Klein tower. The lowest order solution with $n = 0$ is simply a theory quadratic in derivatives of ρ_0, i.e., we have the action of a massless scalar field! In other words, in our four dimensional Minkowski space, we "see" the change in size of the extra dimension as we move from place to place and in time as the changing value of a massless scalar field.

Including more physics, the field ρ_0 can also pick up a small mass, like in the examples of small "explicit symmetry breaking" discussed in previous sections, giving a perfect arena for UBDM to emerge. In a more complex example, we could envisage extra dimensions with weird and wonderful topologies beyond $\mathcal{S}^1$. In this case we require many fields like ρ to describe the compact space, and these fields are called *moduli*. Our metric, Eq. (2.126), made a particular symmetry assumption with no "off-diagonal" components. If we include these, as in the original Kaluza–Klein theory, we obtain new vector fields (i.e., hidden photons) in four dimensions. In string theory, there can be many hundreds of such fields. Finally, if we add supersymmetry and other string theory physics into the mix, then we end up not just with scalars but also with pseudoscalar ALPs and many other weird and wonderful fields that "come along for the ride."

2.6 Non-thermal Production of UBDM

As discussed previously, due to the very small mass of UBDM candidates, cold populations that can provide all the dark matter of the Universe must be created out-of-equilibrium. If thermally produced [94], such particles will have too high a kinetic energy to serve as cold dark matter. Cold populations of UBDM can be produced via a non-equilibrium process known as vacuum misalignment [95–98]. When inflation causes the UBDM field to be homogeneous within our horizon, vacuum misalignment is the dominant production mechanism for UBDM particles. If the UBDM candidate is the product of a phase transition which occurs after inflation, the production of the UBDM particle from cosmic strings and domain walls must also be considered (which is, in essence, another form of vacuum misalignment, but for the UBDM field as a whole).

2.6.1 Vacuum Misalignment

The essence of the vacuum misalignment mechanism is that the initial value of the field is different from the minimum of the field's potential, the vacuum expectation value. When this occurs, the field can oscillate around the minimum of the potential, and the energy density in the oscillating field is the UBDM. This process is commonly called *vacuum misalignment*, as the initial value of the field is misaligned with the potential minimum. (The process is also referred to as vacuum realignment in the literature.)

On large scales, the Universe is known to be isotropic, homogeneous, and expanding, which means it can be described by a Friedmann–Robertson–Walker (FRW) metric, i.e.,

$$-ds^2 = -dt^2 + R^2(t)d\mathbf{x}\cdot d\mathbf{x}\,, \tag{2.129}$$

where $(t, \mathbf{x})$ are co-moving coordinates and $R(t)$ is the scale factor. For a scalar field, ϕ, with an effective potential, $V(\phi)$, the equation of motion can be derived by writing the Lagrangian using the FRW metric instead of the metric for flat spacetime, yielding:

$$\left(\frac{\partial^2}{\partial t^2} + 3\frac{\dot{R}(t)}{R(t)}\frac{\partial}{\partial t} - \frac{1}{R^2(t)}\nabla^2\right)\phi(t,\mathbf{x}) + \frac{\partial V}{\partial \phi} = 0\,. \tag{2.130}$$

In the case of the hidden photon dark matter candidate, we will shortly discuss that the spatial parts of the vector boson field obey an equation of this form. Equation (2.130) is the equation of a harmonic oscillator in an FRW spacetime. When the field is homogeneous over the scale of interest, the spatial derivative in Eq. (2.130) can be neglected. Identifying the Hubble parameter, $H(t) = \dot{R}(t)/R(t)$ (determined from the energy density of radiation in the early universe), the resulting equation is

$$\left(\frac{\partial^2}{\partial t^2} + 3H(t)\frac{\partial}{\partial t}\right)\phi(t,\mathbf{x}) + \frac{\partial V}{\partial \phi} = 0\,. \tag{2.131}$$

When the condition

$$\frac{3}{2}H(t) \gg \sqrt{\frac{1}{\phi}\frac{\partial V}{\partial \phi}} \tag{2.132}$$

is met, the field is overdamped and does not oscillate. Essentially, one wavelength of the field does not fit inside the horizon, and the field is thus "frozen in" and unable to oscillate. When the potential meets the criterion

$$\frac{3}{2}H(t) \simeq \sqrt{\frac{1}{\phi}\frac{\partial V}{\partial \phi}}\,, \tag{2.133}$$

a wavelength of the field is contained within the horizon, and it becomes free to oscillate. The energy in these oscillations is determined by the initial condition, which is the displacement, or misalignment, of the field from the potential minimum (see discussion in the tutorial at the end of Sect. 2.3, where the potential develops a periodic dependence on the phase angle θ describing the bosonic field due to explicit symmetry breaking). We denote this angle θ_i, which corresponds to a field value ϕ_i. The field can relax so that the rms value is zero, and the vacuum is effectively realigned.

2.6.2 *Vector Field Misalignment*

For a vector UBDM candidate arising from kinetic mixing, a phase transition does not occur and a cold population of hidden photons can be entirely produced by vacuum misalignment. While this mechanism was originally discussed in terms of the axion [95–97], we will cover the hidden photon here first, as it is a more simple case. That the spatial component of a light vector boson can also satisfy Eq. (2.131) and result in a cold population was first discussed in Ref. [98].

The hidden photon field, $\mathcal{X}_\mu$, will be uniform over the scale of the horizon after inflation, with an initial random value. As it is spatially uniform, $\partial_i \mathcal{X}_\mu \sim 0$, and the resulting equation of motion is [98]

$$\left(\frac{\partial^2}{\partial t^2} + 3H(t)\frac{\partial}{\partial t}\right)\mathcal{X}_i(\mathbf{x}) + m_{\gamma'}^2 \mathcal{X}_i(\mathbf{x}) = 0 \tag{2.134}$$

with the mass term giving an effective potential when $m_{\gamma'} \neq 0$. When the condition of Eq. (2.133) is met and $H(t) \sim m_{\gamma'}$, the field can begin to oscillate and act as cold dark matter.

A simple bound on $m_{\gamma'}$ can be obtained by requiring that the particle's Compton wavelength permit structure formation on kiloparsec scales [98, 99]. Then the requirement that 1 kpc $< \hbar/\left(m_{\gamma'} v_{\rm esc}\right)$, where $v_{\rm esc}$ is the escape velocity of the structure, gives a bound $m_{\gamma'}c^2 \geq 1.7 \times 10^{-24}$ eV. More detailed bounds can be obtained from considering decays, interactions of the hidden photon with other particles, and experimental observations [98]. Further discussion is in Chap. 3.

2.6.3 Scalar Field Misalignment

For scalar (or pseudoscalar) fields that occur as the pseudo-Nambu-Goldstone boson, such as axions and ALPs, there are two temperature scales that govern the non-equilibrium production mechanisms of the particles in the early Universe. These are the temperature at which spontaneous symmetry breaking occurs, T_{SB}, and the temperature at which the boson field acquires an effective potential, T_{eff}. For the QCD axion, T_{SB} is the temperature at which the Peccei-Quinn symmetry is spontaneously broken, T_{PQ}. In addition to vacuum misalignment, other topological effects may contribute to the cold population of axions in the Universe, depending on the relationship between T_{PQ} and the inflationary reheating temperature, T_R. For ALPs from string models, T_{SB} is the Kaluza–Klein scale,[10] generally assumed to be far above the inflationary reheating temperature. Thus, for ALPs it is commonly accepted that vacuum misalignment is the method by which a potential ALP dark matter population is produced in the early Universe.

In the scalar cases, at T_{SB}, a global chiral symmetry is spontaneously broken, and the phase can take on any value, θ_i. If $T_{SB} > T_R$, a value of the initial misalignment angle in one region of space can be inflated such that the misalignment angle has the same value everywhere within the horizon. In this case, non-equilibrium production of the scalar particles is similar to that of a cold population of hidden photons occurring due to vacuum misalignment as discussed in Sect. 2.6.2. For axions, if $T_{PQ} < T_R$, fluctuations in local temperature mean that spontaneous symmetry breaking will be seeded at different locations within the horizon, and each location will select a different value of ϕ_i. At the interface of regions with different ϕ_i, topological axion strings and domain walls will occur. These are not observed, so we surmise that they have decayed via the various available channels. In the following, we will discuss vacuum misalignment in detail, similar to Ref. [100], and touch on the other production mechanisms. A more in-depth discussion of axion cosmology is given by Ref. [101]. In the following, we will refer to the axion, but the discussion also applies to ALPs.

The second temperature scale for the axion, T_{eff}, is when a significant mass term for the axion arises. The chiral anomaly couples the axion to the gauge field, and the gauge field instantons induce a potential and hence a mass for the axion through soft explicit symmetry breaking (following the basic ideas discussed in Sect. 2.3). This occurs at the scale when the quark-gluon plasma condenses to hadrons. We denote this time t_1 and at this temperature, $m_a t_1 \sim 1$ [95–97]. Note that $T_{QCD} \simeq 1$ GeV. For ALPs from string theory, similar non-perturbative effects create a potential for the ALP and, consequently, a mass.

When m_a becomes significant, the axion field gains an effective periodic potential, analogous to that described by Eq. (2.54),

[10] The Kaluza–Klein scale is the energy scale associated with the size of the compactified or "curled-up" extra dimensions in string theory [88].

$$V(\phi) = m_a^2(T) f_a^2 \left(1 - \cos\left(\frac{\phi}{f_a}\right)\right) = m_a^2(T) f_a^2 (1 - \cos\theta) \ , \tag{2.135}$$

where $\theta = \phi/f_a$. At low temperatures, the axion mass is given by Eq. (2.115)

$$m_a \simeq 6 \times 10^{-6} \text{ eV} \left(\frac{10^{12} \text{ GeV}}{f_a}\right) \ ,$$

as discussed in the tutorial at the end of Sect. 2.5.1. At higher temperatures—while the potential is effectively "turning on"—the axion mass has a temperature dependence (which can be calculated using lattice QCD, see discussion in Ref. [75]).

Using the effective potential given by Eq. (2.135) with Eq. (2.131), the equation of motion governing the axion field dynamics is

$$\left(\frac{\partial^2}{\partial t^2} + 3H(t)\frac{\partial}{\partial t}\right)\phi(t, \mathbf{x}) + m_a^2(T(t)) f_a \sin\theta = 0 \ . \tag{2.136}$$

The dependence of temperature on time in the early universe is discussed in Chap. 3. Using Eq. (2.136), the density of cold axions can be estimated as follows. For small oscillations near $\theta = 0$, $\sin\theta \approx \theta$ and

$$\left(\frac{\partial^2}{\partial t^2} + 3H(t)\frac{\partial}{\partial t}\right)\phi(t, \mathbf{x}) + m_a^2(t)\phi(t, \mathbf{x}) = 0 \ . \tag{2.137}$$

At temperatures above T_{eff}, θ is approximately constant, and m_a can be neglected. When $m_a t_1 \sim 1$, the field begins to oscillate, which corresponds to the time [101]

$$t_1 \simeq 2 \times 10^{-7} \text{ s} \left(\frac{f_a}{10^{12} \text{ GeV}}\right)^{\frac{1}{3}} \tag{2.138}$$

and

$$T_{\text{eff}} \simeq 1 \text{ GeV} \left(\frac{10^{12} \text{ GeV}}{f_a}\right)^{\frac{1}{6}} \ . \tag{2.139}$$

Alignment of the field will occur on the order of the same timescale, and thus its momentum is on the order of

$$p_a(t_1) \sim \frac{1}{t_1} \ . \tag{2.140}$$

If $f_a \sim 10^{12}$ GeV, then $m_a \sim 6$ μeV, and the field momentum will be $p_a \sim 10^{-9}$ eV. From this estimate, it is easily seen that the initial momentum of a

population of axions from vacuum misalignment is much less than the axion mass, thus the population is nonrelativistic, or cold.

The question of whether or not a sufficient number of axions are produced to account for all the dark matter in the Universe can be addressed by estimating the energy density. Expanding around the potential minimum, this density is

$$\rho = \frac{f_a^2}{2}\left(\dot{\theta}^2 + m_a^2(t)\theta^2\right) . \tag{2.141}$$

The virial theorem gives

$$\langle\dot{\theta}^2\rangle = m_a^2\langle\theta^2\rangle = \frac{\rho}{f_a^2} . \tag{2.142}$$

The energy density of these nonrelativistic axions (for the given potential) scales with the expansion of the Universe (see Problem 3.1) as

$$\rho \propto \frac{m_a(t)}{R^3(t)}. \tag{2.143}$$

For the initial misalignment angle, θ_i, the energy density in coherent axion oscillations is

$$\rho_i = \frac{1}{2}m_a^2(t_1)f_a^2\theta_i^2 = \frac{1}{2}m_a^2(t_1)\phi_i^2 . \tag{2.144}$$

Given matter dominated expansion of the Universe until today, the axion density scales with Eq. (2.143), to give today's average axion density,

$$\rho_0 \sim \rho_i \frac{m_a(t_0)}{m_a(t_i)}\frac{R^3(t_i)}{R^3(t_0)} , \tag{2.145}$$

or

$$\rho_0 \sim \frac{1}{2}f_a^2\frac{m_a}{t_1}\frac{R^3(t_1)}{R^3(t_0)}\phi_i^2 , \tag{2.146}$$

using Eq. (2.144) and $m_a t_1 \sim 1$. The initial misalignment angle, θ_i, has a single value if T_{PQ} is greater than the inflationary reheat temperature, T_R. In the case when $T_{PQ} < T_R$, ϕ_i can have several different values within the horizon, and additionally, higher-order modes of Eq. (2.136) can be occupied. Under these circumstances, Eq. (2.146) gives the correct expression for the zero-momentum mode if we replace θ_i with its average within the horizon, expected to be $O(1)$. Using Eqs. (2.115), (2.138), and (2.139), and assuming $m_a(T) \propto T^{-4}$, the energy density in axions from this population today is

$$\Omega_a \sim \left(\frac{f_a}{10^{12}\ \text{GeV}}\right)^{\frac{7}{6}} . \tag{2.147}$$

For $T_{PQ} > T_R$ and $\theta_i \sim 1$, this gives the cold axion population today. For $T_{PQ} < T_R$, it is expected that there is an equal contribution from the sum of all higher-order modes, and possible contributions from string and wall decay. A thorough discussion of all these contributions can be found in Ref. [101].

References

1. T. Lancaster, S.J. Blundell, *Quantum Field Theory for the Gifted Amateur* (Oxford University Press, Oxford, 2014)
2. A. Zee, *Quantum Field Theory in a Nutshell*, vol. 7 (Princeton University Press, Princeton, 2010)
3. S. Weinberg, *The Quantum Theory of Fields*, vol. 1–2 (Cambridge University Press, Cambridge, 1995)
4. M. Peskin, *An Introduction to Quantum Field Theory* (CRC Press, Boca Raton, 2018)
5. M. Srednicki, *Quantum Field Theory* (Cambridge University Press, Cambridge, 2007)
6. G. Aad, T. Abajyan, B. Abbott, J. Abdallah, S.A. Khalek, A.A. Abdelalim, R. Aben, B. Abi, M. Abolins, O. AbouZeid, et al., Phys. Lett. B **716**, 1 (2012)
7. S. Chatrchyan, V. Khachatryan, A.M. Sirunyan, A. Tumasyan, W. Adam, E. Aguilo, T. Bergauer, M. Dragicevic, J. Erö, C. Fabjan, et al., Phys. Lett. B **716**, 30 (2012)
8. G. Aad, T. Abajyan, B. Abbott, J. Abdallah, S.A. Khalek, R. Aben, B. Abi, M. Abolins, O. AbouZeid, H. Abramowicz, et al., Phys. Lett. B **726**, 120 (2013)
9. T. Clifton, P.G. Ferreira, A. Padilla, C. Skordis, Phys. Rep. **513**, 1 (2012)
10. G. Sardanashvily, *Noether's Theorems* (Springer, Berlin, 2016)
11. S.R. Choudhury, S. Choubey, J. Cosmol. Astropart. Phys. **2018**, 017 (2018)
12. C.P. Burgess, Phys. Rep. **330**, 193 (2000)
13. J. Goldstone, A. Salam, S. Weinberg, Phys. Rev. **127**, 965 (1962)
14. R. Peccei, Lect. Notes Phys. **741**, 3 (2008)
15. L.D. Duffy, K. Van Bibber, New J. Phys. **11**, 105008 (2009)
16. J.E. Kim, G. Carosi, Rev. Mod. Phys. **82**, 557 (2010)
17. P. Sikivie, Comptes Rendus Physique **13**, 176 (2012)
18. P. Arias, D. Cadamuro, M. Goodsell, J. Jaeckel, J. Redondo, A. Ringwald, J. Cosm. Astropart. Phys. **2012**, 013 (2012)
19. P.W. Graham, I.G. Irastorza, S.K. Lamoreaux, A. Lindner, K.A. van Bibber, Ann. Rev. Nucl. Part. Sci. **65**, 485 (2015)
20. P.W. Graham, D.E. Kaplan, J. Mardon, S. Rajendran, W.A. Terrano, Phys. Rev. D **93**, 075029 (2016)
21. D.J. Gross, R.D. Pisarski, L.G. Yaffe, Rev. Mod. Phys. **53**, 43 (1981)
22. M. Dine, P. Draper, L. Stephenson-Haskins, D. Xu, Phys. Rev. D **96**, 095001 (2017)
23. T. Damour, G. Gibbons, C. Gundlach, Phys. Rev. Lett. **64**, 123 (1990)
24. M. Safronova, D. Budker, D. DeMille, D.F. Jackson Kimball, A. Derevianko, C.W. Clark, Rev. Mod. Phys. **90**, 025008 (2018)
25. C.S. Wu, E. Ambler, R. Hayward, D. Hoppes, R.P. Hudson, Phys. Rev. **105**, 1413 (1957)
26. J.H. Christenson, J.W. Cronin, V.L. Fitch, R. Turlay, Phys. Rev. Lett. **13**, 138 (1964)
27. L. Barkov, M. Zolotorev, JETP Lett. **27**, 357 (1978)
28. L. Barkov, M. Zolotorev, JETP Lett. **28**, 50 (1978)
29. R. Conti, P. Bucksbaum, S. Chu, E. Commins, L. Hunter, Phys. Rev. Lett. **42**, 343 (1979)

30. J.D. Jackson, *Classical Electrodynamics*, 2nd edn. (Wiley, New York, 1975)
31. H. Primakoff, Phys. Rev. **81**, 899 (1951)
32. P. Sikivie, Phys. Rev. Lett. **51**, 1415 (1983)
33. P. Sikivie, Phys. Rev. D **32**, 2988 (1985)
34. J. Ouellet, Z. Bogorad, Phys. Rev. D **99**, 055010 (2019)
35. Y. Kim, D. Kim, J. Jeong, J. Kim, Y.C. Shin, Y.K. Semertzidis, Phys. Dark Universe **26**, 100362 (2019)
36. G.B. Arfken, H.J. Weber, *Mathematical Methods for Physicists* (Elsevier, Amsterdam, 1999)
37. M.L. Boas, *Mathematical Methods in the Physical Sciences* (Wiley, Hoboken, 2006)
38. D. Budker, P.W. Graham, M. Ledbetter, S. Rajendran, A.O. Sushkov, Phys. Rev. X **4**, 021030 (2014)
39. N. Crescini, D. Alesini, C. Braggio, G. Carugno, D. D'Agostino, D. Di Gioacchino, P. Falferi, U. Gambardella, C. Gatti, G. Iannone, et al., Phys. Rev. Lett. **124**, 171801 (2020)
40. M. Pospelov, S. Pustelny, M.P. Ledbetter, D.F. Jackson Kimball, W. Gawlik, D. Budker, Phys. Rev. Lett. **110**, 021803 (2013)
41. S. Pustelny, D.F. Jackson Kimball, C. Pankow, M.P. Ledbetter, P. Wlodarczyk, P. Wcislo, M. Pospelov, J.R. Smith, J. Read, W. Gawlik, D. Budker, Ann. Phys. **525**, 659 (2013)
42. A. Arvanitaki, A.A. Geraci, Phys. Rev. Lett. **113**, 161801 (2014)
43. D. Budker, P.W. Graham, M. Ledbetter, S. Rajendran, A.O. Sushkov, Phys. Rev. X **4**, 021030 (2014)
44. T. Wu, J.W. Blanchard, G.P. Centers, N.L. Figueroa, A. Garcon, P.W. Graham, D.F. Jackson Kimball, S. Rajendran, Y.V. Stadnik, A.O. Sushkov, et al., Phys. Rev. Lett. **122**, 191302 (2019)
45. A. Garcon, J.W. Blanchard, G.P. Centers, N.L. Figueroa, P.W. Graham, D.F. Jackson Kimball, S. Rajendran, A.O. Sushkov, Y.V. Stadnik, A. Wickenbrock, et al., Sci. Adv. **5**, eaax4539 (2019)
46. S. Afach, D. Budker, G. DeCamp, V. Dumont, Z.D. Grujić, H. Guo, D.F. Jackson Kimball, T. Kornack, V. Lebedev, W. Li, et al., Phys. Dark Universe **22**, 162 (2018)
47. R. Peccei, H.R. Quinn, Phys. Rev. Lett. **38**, 1440 (1977)
48. R. Peccei, H.R. Quinn, Phys. Rev. D **16**, 1791 (1977)
49. P.W. Graham, D.E. Kaplan, S. Rajendran, Phys. Rev. Lett. **115**, 221801 (2015)
50. K. Harigaya, et al., Phys. Rev. Lett. **124**, 111602 (2020)
51. R.T. Co, L.J. Hall, K. Harigaya, J. High Energ. Phys. **2021**, 172 (2021)
52. P. Svrcek, E. Witten, J. High Energy Phys. **06**, 051 (2006)
53. A. Arvanitaki, S. Dimopoulos, S. Dubovsky, N. Kaloper, J. March-Russell, Phys. Rev. D **81**, 123530 (2010)
54. B. Holdom, Phys. Lett. B **166**, 196 (1986)
55. M. Cvetic, P. Langacker, Phys. Rev. D **54**, 3570 (1996)
56. S. Weinberg, Phys. Rev. Lett. **40**, 223 (1978)
57. F. Wilczek, Phys. Rev. Lett. **40**, 279 (1978)
58. C. Abel, S. Afach, N.J. Ayres, C.A. Baker, G. Ban, G. Bison, K. Bodek, V. Bondar, M. Burghoff, E. Chanel, et al., Phys. Rev. Lett. **124**, 081803 (2020)
59. T. Chupp, P. Fierlinger, M. Ramsey-Musolf, J. Singh, Rev. Mod. Phys. **91**, 015001 (2019)
60. B. Graner, Y. Chen, E. Lindahl, B. Heckel, et al., Phys. Rev. Lett. **116**, 161601 (2016)
61. J.E. Kim, Phys. Rep. **150**, 1 (1987)
62. H.Y. Cheng, Phys. Rep. **158**, 1 (1988)
63. M.S. Turner, Phys. Rep. **197**, 67 (1990)
64. G.G. Raffelt, Phys. Rep. **198**, 1 (1990)
65. J. de Vries, E. Mereghetti, A. Walker-Loud, Phys. Rev. C **92**, 045201 (2015)
66. J. Bsaisou, J. de Vries, C. Hanhart, S. Liebig, U.G. Meißner, D. Minossi, A. Nogga, A. Wirzba, J. High Energy Phys. **2015**, 104 (2015)
67. S.L. Adler, Phys. Rev. **177**, 2426 (1969)
68. J. Bell, R. Jackiw, Nuovo Cim. A **60**, 47 (1969)
69. S. Kanemaki, I. Furuoya, Prog. Theor. Phys. **89**, 1235 (1993)

70. W.A. Bardeen, S.H. Tye, Phys. Lett. B **74**, 229 (1978)
71. L. Di Luzio, M. Giannotti, E. Nardi, L. Visinelli, Phys. Rep. **870**, 1 (2020)
72. G.G. di Cortona, E. Hardy, J.P. Vega, G. Villadoro, J. High Energy Phys. **2016**, 34 (2016)
73. D.J. Gross, R.D. Pisarski, L.G. Yaffe, Rev. Mod. Phys. **53**, 43 (1981)
74. O. Wantz, E.P.S. Shellard, Phys. Rev. D **82**, 123508 (2010)
75. S. Borsanyi, et al., Nature **539**, 69 (2016)
76. H. Davoudiasl, C.W. Murphy, Phys. Rev. Lett. **118**, 141801 (2017)
77. G. Degrassi, S. Di Vita, J. Elias-Miro, J.R. Espinosa, G.F. Giudice, G. Isidori, A. Strumia, J. High Energy Phys. **2012**, 98 (2012)
78. Y. Hamada, H. Kawai, K.Y. Oda, Phys. Rev. D **87**, 053009 (2013)
79. J. Elias-Miro, J.R. Espinosa, G.F. Giudice, G. Isidori, A. Riotto, A. Strumia, Phys. Lett. B **709**, 222 (2012)
80. S. Dimopoulos, H. Georgi, Nucl. Phys. B **193**, 150 (1981)
81. N. Arkani-Hamed, S. Dimopoulos, G.R. Dvali, Phys. Lett. B **429**, 263 (1998)
82. L. Randall, R. Sundrum, Phys. Rev. Lett. **83**, 3370 (1999)
83. N. Fonseca, E. Morgante, Phys. Rev. D **100**, 055010 (2019)
84. A. Banerjee, H. Kim, G. Perez, Phys. Rev. D **100**, 115026 (2019)
85. R. Gupta, J. Reiness, M. Spannowsky, Phys. Rev. D **100**, 055003 (2019)
86. R.S. Gupta, Z. Komargodski, G. Perez, L. Ubaldi, J. High Energy Phys. **2016**, 166 (2016)
87. J. Espinosa, C. Grojean, G. Panico, A. Pomarol, O. Pujolas, G. Servant, Phys. Rev. Lett. **115**, 251803 (2015)
88. B. Zwiebach, *A First Course in String Theory* (Cambridge University Press, Cambridge, 2004)
89. E. Witten, Nucl. Phys. B **186**, 412 (1981)
90. J.M. Overduin, P.S. Wesson, Phys. Rep. **283**, 303 (1997)
91. L. Randall, R. Sundrum, Phys. Rev. Lett. **83**, 3370 (1999)
92. L. Randall, R. Sundrum, Phys. Rev. Lett. **83**, 4690 (1999)
93. D.Z. Freedman, A. Van Proeyen, *Supergravity* (Cambridge University Press, Cambridge, 2012)
94. E.W. Kolb, M.S. Turner, Nature **294**, 521 (1981)
95. L. Abbott, P. Sikivie, Phys. Lett. B **120**, 133 (1983)
96. J. Preskill, M.B. Wise, F. Wilczek, Phys. Lett. B **120**, 127 (1983)
97. M. Dine, W. Fischler, Phys. Lett. B **120**, 137 (1983)
98. A.E. Nelson, J. Scholtz, Phys. Rev. D **84**, 103501 (2011)
99. P. van Dokkum, et al., Astrophys. J. Lett. **677**, L5 (2008)
100. L.D. Duffy, K. van Bibber, New J. Phys. **11**, 105008 (2009)
101. P. Sikivie, Lect. Notes Phys. **741**, 19 (2008)